

# Survey of Radar Signal Processing

G. V. TRUNK  
*Radar Analysis Staff*  
*Radar Division*

June 21, 1977



**NAVAL RESEARCH LABORATORY**  
Washington, D.C.

Approved for public release; distribution unlimited.

REPORT DOCUMENTATION PAGE		READ INSTRUCTIONS BEFORE COMPLETING FORM
1. REPORT NUMBER NRL REPORT 8117	2. GOVT ACCESSION NO.	3. RECIPIENT'S CATALOG NUMBER
4. TITLE (and Subtitle) SURVEY OF RADAR SIGNAL PROCESSING		5. TYPE OF REPORT & PERIOD COVERED Final Report on one phase of a continuing NRL Problem
		6. PERFORMING ORG. REPORT NUMBER
7. AUTHOR(s) G. V. Trunk		8. CONTRACT OR GRANT NUMBER(s)
9. PERFORMING ORGANIZATION NAME AND ADDRESS Naval Research Laboratory Washington, D. C. 20375		10. PROGRAM ELEMENT, PROJECT, TASK AREA & WORK UNIT NUMBERS NRL Problem R02-97 Program Element 61153N Project RR021-05-41
11. CONTROLLING OFFICE NAME AND ADDRESS Department of the Navy Office of Naval Research Arlington, Va. 22217		12. REPORT DATE June 21, 1977
		13. NUMBER OF PAGES 48
14. MONITORING AGENCY NAME & ADDRESS (if different from Controlling Office)		15. SECURITY CLASS. (of this report) Unclassified
		15a. DECLASSIFICATION/DOWNGRADING SCHEDULE
16. DISTRIBUTION STATEMENT (of this Report)  Approved for public release; distribution unlimited		
17. DISTRIBUTION STATEMENT (of the abstract entered in Block 20, if different from Report)		
18. SUPPLEMENTARY NOTES		
19. KEY WORDS (Continue on reverse side if necessary and identify by block number)		
Coherent processing	Noncoherent detection	Tracking filters
Sidelobe cancelers	Integrators	Correlation logic
Adaptive radars	Adaptive thresholding	Radar integration
MTI	Nonparametric detectors	
Doppler processing	Track-while-scan	
20. ABSTRACT (Continue on reverse side if necessary and identify by block number)		
<p>During the last decade, considerable progress has been made in radar signal processing, and this report states its present status. The three broad areas of coherent processing, noncoherent detection, and track-while-scan systems are discussed.</p> <p>Specifically, in the area of coherent processing the subjects of sidelobe cancelers, adaptive radars, MTIs, and doppler processing are discussed. In the adaptive processing area, both the maximum signal-to-noise and least mean-square methods are described, and special emphasis is given to</p> <p style="text-align: right;">(Continued)</p>		

DD FORM 1473  
1 JAN 73EDITION OF 1 NOV 65 IS OBSOLETE  
S/N 0102-LF-014-6601

SECURITY CLASSIFICATION OF THIS PAGE (When Data Entered)

## 20. ABSTRACT (Continued)

the problem of convergent rate. The moving-target detector (MTD) is used as an example of doppler processing.

In the area of noncoherent detection, various integrators are discussed. Among these are the moving window, feedback integrator, two-pole filter, binary integrator, and batch processor. Methods of obtaining a constant false-alarm rate using either adaptive thresholding or nonparametric detectors are also considered.

A general outline of a track-while-scan system is considered first. Then, detailed discussions of the tracking filter, maneuver-following logic, track initiation, and correlation logic are presented. Finally, methods of integrating data from several radars are discussed.

## CONTENTS

INTRODUCTION .....	1
COHERENT PROCESSING .....	1
Sidelobe Cancelers .....	2
Adaptive Arrays and Radars .....	6
Moving-Target Indicators .....	14
Doppler Processing .....	18
Noncoherent MTI Indicators .....	19
NONCOHERENT DETECTION .....	20
Classical Theory .....	20
Integrators .....	22
Moving Window .....	22
Feedback Integrator .....	23
Two-Pole Filter .....	24
Binary Integrator .....	24
Batch Processor .....	24
False Alarms .....	25
Adaptive Thresholding .....	26
Nonparametric Detectors .....	28
Sequential Detectors .....	30
TRACKING SYSTEM .....	31
System Outline .....	32
Tracking Filters .....	33
Maneuver-Following Logic .....	35
Track Initiation .....	38
Correlation Logic .....	38
Radar Integration .....	41
CONCLUDING REMARKS .....	44

# SURVEY OF RADAR SIGNAL PROCESSING

## INTRODUCTION

During the last decade considerable progress has been made in radar signal processing. This progress is directly traceable to the lowered cost and increased speed of digital hardware and computers and to more sophisticated techniques in adaptive processing and tracking systems.

This survey of radar signal processing will neglect waveform design and include the track-while-scan systems. Waveform design will be neglected because it has received considerable attention elsewhere, with the books of Rihaczek\* and Cook and Bernfeld† covering the subject in detail. On the other hand, although track-while-scan systems properly fall under the heading of radar data processing, it does not make sense to have an automatic detection system unless it is accompanied by a tracking system. Therefore, since tracking is a necessary part of the entire system, the survey will include it.

Thus this survey of radar signal processing will consider the three broad areas of coherent processing (processing of amplitude and phase), noncoherent processing (processing of amplitude), and track-while-scan systems. The subjects will be discussed in the same order as the radar signal passes through the radar system. Specifically, in the area of coherent processing the subjects of sidelobe cancelers, adaptive antennas, and MTIs (moving-target indicators) will be covered. In the area of noncoherent detection, methods of obtaining a constant false-alarm rate (CFAR) using either adaptive thresholding or nonparametric detectors will be emphasized. The section on the tracking system will cover the tracking filter, correlation logic, track initiations, maneuver-following logic, and a basic overview of an entire tracking system.

## COHERENT PROCESSING

In the area of coherent processing, adaptive processing will receive considerable attention. There are two approaches to adaptive processing: the method of maximum signal-to-noise ratio (S/N) due to Howells‡ and Applebaum§ and the least-mean-square method (LMS) due to Widrow and Hoff#. The two methods, although appearing quite different, yield almost equivalent results. So that both methods will be presented, the LMS method will be used during discussion of sidelobe cancelers, and the method of maximum S/N will be used during discussion of adaptive arrays and radars. For adaptive radars special consideration will be given to

---

\*A. W. Rihaczek, *Principles of High-Resolution Radar*, McGraw-Hill, New York, 1969.

†C. E. Cook and M. Bernfeld, *Radar Signals, An Introduction to Theory and Application*, Academic Press, New York, 1967.

‡P. W. Howells, IEEE Trans. Antennas and Propagation AP-24, 575-584 (1976).

§S. P. Applebaum, IEEE Trans. Antennas and Propagation AP-24, 585-598 (1976).

#B. Widrow and M. E. Hoff, IRE WESCON Conv. Rec., 96-104, 1960.

the problem of convergent rate. Finally, MTIs will be discussed and the moving-target-detector (MTD) system will be used as an example of doppler processing.

### Sidelobe Cancelers

The basic idea of a sidelobe canceler (a device that attempts to eliminate interference entering through the antenna sidelobes) is shown in Fig. 1. The signal  $S$  of interest enters through the main lobe of the antenna, and the jamming (interfering signal), which is much stronger than the signal of interest, enters through the sidelobe of the main antenna. The auxiliary antenna is an omnidirectional antenna, and it will be assumed that the signal entering the omnidirectional antenna is much smaller than the jamming  $J_a$  and can be neglected, since the signal and jamming now have the same antenna gain. (The treatment of the signal in the auxiliary channel can be found in Widrow et al.)\* The adaptive filter produces an output  $Y$  which is as close as possible to the input jamming  $J$ . The filter output is then subtracted from the main input, producing an output  $Z = S + J - Y$ . If the filter output is an exact replica of  $J$ , the output is the desired signal  $S$ .

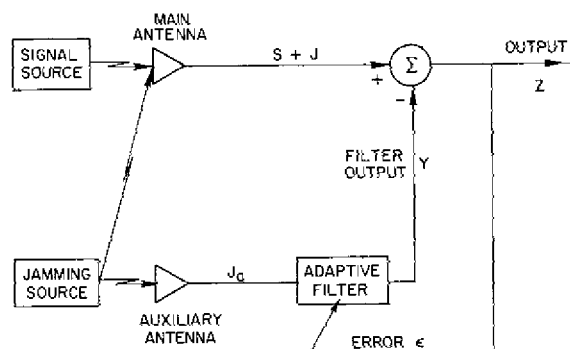


Fig. 1 — Concept of adaptive noise canceling

The filter is controlled by adjusting its parameters to minimize the output power. To show that this minimization will force  $Y$  to be a replica of  $J$ , a development in Widrow et al.\* is repeated. First, assume  $S$ ,  $J$ , and  $J_a$  are zero-mean random variables,  $S$  is uncorrelated with  $J$  and  $J_a$ , and  $J_a$  (and hence  $Y$ ) is correlated with  $J$ . The expected output power is

$$E\{Z^2\} = E\{S^2\} + E\{(J - Y)^2\} + 2E\{S(J - Y)\} = E\{S^2\} + E\{(J - Y)^2\}. \quad (1)$$

Adjusting the filter to minimize  $E\{Z^2\}$  is equivalent to minimizing  $E\{(J - Y)^2\}$ , since  $Y$  is uncorrelated with  $S$ ; that is,  $Y$  is the best least-squares estimate of the jamming  $J$ . Furthermore, since  $Z - S = J - Y$ , minimizing  $E\{(J - Y)^2\}$  causes  $Z$  to be the best least-squares estimate of the signal  $S$ .

The adaptive filter for obtaining a least-squares estimate of a desired signal  $S$  can be described by a weighting vector  $W$ , where  $W^T = (W_1, W_2, \dots, W_n)$  and  $T$  denotes the transpose, operating on the input  $J_a = X$ ,  $X^T = (x_1, \dots, x_n)$ . Thus the filter output is

$$Y = X^T W, \quad (2)$$

\*B. Widrow, J. R. Glover, Jr., J. M. McCool, J. Kaunitz, C. S. Williams, R. H. Hearn, J. R. Zeidler, E. Dong, Jr., and R. C. Goodlin, Proc. IEEE 63, 1692-1716 (1975).

and the error, defined as the difference between the input signal and the filter output, is

$$\epsilon = S + J - X^T W. \quad (3)$$

The least-mean-square (LMS) adaptive filter adjusts the weighting vector  $W$  to minimize the mean-square error. The squared error is

$$\epsilon^2 = (S + J)^2 - 2(S + J)X^T W + W^T X X^T W. \quad (4)$$

Taking the expected value of (4), letting the vector  $P$  be the crosscorrelation between  $J$  and  $X$  ( $P = E\{JX\}$ ), and letting the matrix  $K$  be the covariance matrix of  $X$  ( $K = E\{XX^T\}$ ), one obtains

$$E\{\epsilon^2\} = E\{S^2\} + E\{J^2\} - 2P^T W + W^T K W. \quad (5)$$

To find the minimum of (5) with respect to  $W$ , the gradient  $\nabla$  of (5) is set to zero, yielding the optimal weight vector

$$W = K^{-1} P. \quad (6)$$

The LMS adaptive algorithm is an iterative method of finding an approximate solution to (6). The algorithm has the advantage of not requiring an explicit measurement of the correlation function or inversion of the covariance matrix. Specifically, the LMS algorithm uses the method of steepest descent to solve (6); that is, the next weight vector  $W_{j+1}$  is equal to the old weight vector plus a step in the direction of the negative gradient:

$$W_{j+1} = W_j - \mu \nabla_j. \quad (7)$$

The gradient of the squared error on the  $j$ th iteration is

$$\nabla_j = \nabla \epsilon_j^2 = \nabla (S + J - X_j^T W_j)^2 = -2\epsilon_j X_j. \quad (8)$$

Thus the next weight is given recursively by

$$W_{j+1} = W_j + 2\mu \epsilon_j X_j \quad (9)$$

and is known as the Widrow-Hoff LMS algorithm. The parameter  $\mu$  is a factor which controls the rate of convergence and the stability of the method. It has been shown\*† that (9) converges to the optimal solution as long as  $\mu$  is between zero and the reciprocal of the largest eigenvalue of the covariance matrix  $K$ . Shown in Fig. 2 is a typical learning curve and an average of 48 learning curves for the LMS algorithm. The average reveals the basic exponential nature of the learning curve. For the radar case  $X_j$  represents the sample from  $j$ th range cell; consequently the number of iterations corresponds to the number of range cells.

In principal, if the situation shown in Fig. 1 is correct (no uncorrelated noise in each channel and no signal in the auxiliary) the jamming can be completely canceled. However, if the situation is as shown in Fig. 3, total cancellation cannot be accomplished. Specifically, the performance of the canceler can be described by the ratio  $R$  of S/N at the output to S/N at the

\*B. Widrow, P. E. Mantey, L. J. Griffiths, and B. B. Goode, Proc. IEEE 55, 2143-2159 (1967).

†R. L. Riegler and R. T. Compton, Jr., Proc. IEEE 61, 748-758 (1973).

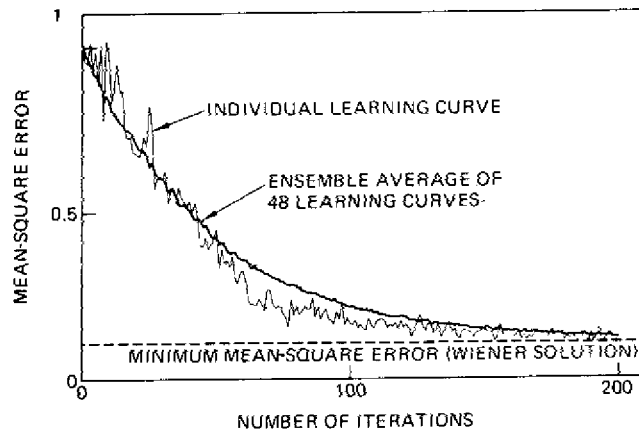


Fig. 2 — Typical learning curves for the LMS algorithm. (From) B. Widrow et al., Proc. IEEE 63, 1692-1716 (1975), courtesy of the Institute of Electrical and Electronics Engineers.)

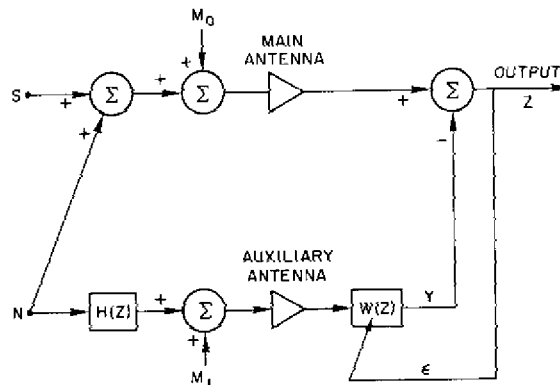


Fig. 3 — Adaptive noise canceler with correlated and uncorrelated noises in the main and auxiliary antennas

primary input (main antenna). Widrow et al.\* have shown that this ratio  $R$  for steady state (after convergence) can be expressed as

$$R = \frac{[A(z) + 1] [B(z) + 1]}{A(z) + A(z) B(z) + B(z)}, \quad (10)$$

where  $A(z)$  and  $B(z)$  are noise-to-noise ratios

$$A(z) = S_0(z)/S_n(z) \quad (11)$$

and

$$B(z) = S_1(z)/S_n(z) |H(z)|^2, \quad (12)$$

\*B. Widrow, J. R. Glover, Jr., J. M. McCool, J. Kaunitz, C. S. Williams, R. H. Hearn, J. R. Zeidler, E. Dong, Jr., and R. C. Goodlin, Proc. IEEE 63, 1692-1716 (1975).

in which  $S_0$ ,  $S_1$ , and  $S_n$  are the power density spectra of the noises  $m_0$ ,  $m_1$ , and  $n$  respectively and  $H(z)$  is the channel transfer function for the correlated noise (jamming). It is obvious from (10) that the cancellation is limited by the uncorrelated noise components in the primary and reference channels. When the jamming is much stronger than the uncorrelated noise components,  $A(z)$  and  $B(z)$  are small and

$$R \simeq \frac{1}{A(z) + B(z)}, \quad (13)$$

giving a large improvement in the output signal-to-jamming ratio. However the improvement indicated by (13) is rarely achieved in practice. Factors limiting performance include the finite time for the adaptive process, the presence of signal components in the auxiliary channel, multipath problems, and misadjustment caused by gradient estimation noise in the adaptive process.\* Furthermore, in theory  $N$  omnidirectional antennas (and associated cancellation loops) are needed to cancel  $N$  jammers. However, because of multipath propagation, the energy from a single jammer can enter the antenna from several directions and for all practical purposes appears to be from several jammers. Therefore in practice one requires several times as many cancellation loops as jammers.

Recently F. Kretschmer and B. Lewis† have developed an improved algorithm for simulation of the Applebaum-Howells adaptive loop and for use in adaptive processing. The LMS algorithm discussed above is given by

$$W_{j+1} = W_j + 2\mu\epsilon_j X_j. \quad (9)$$

This is commonly used to simulate and analyze the Applebaum-Howells adaptive loop in the form

$$W_{j+1} = kW_j + G(1 - k)\epsilon_j X_j^*, \quad (14)$$

where  $k = 1 - 1/\tau$ , with  $\tau$  being the filter smoothing constant, and  $G$  being the gain term. Thus in both algorithms the next weight is derived in terms of the present error and sample. Kretschmer and Lewis point out that for fast loops  $W_{j+1}$  as given by (9) and (14) is not the proper weight. Rather, for better cancellation and more realistic canceler loop simulation,  $W_{j+1}$  should be calculated from

$$W_{j+1} = W_j + 2\mu\epsilon_{j+1} X_{j+1}^*. \quad (15)$$

In effect, by using the sample  $X_j$  to calculate the weight  $W_{j+1}$ , a phase shift is introduced which can result in loop instability. Kretschmer and Lewis have shown (for the Applebaum-Howells application) that the stability condition of the LMS algorithm is

$$|G(1 - k)|X_j|^2 - k| < 1 \quad (16)$$

and that their improved algorithm is unconditionally stable.

Comparison of the LMS algorithm with the improved algorithm was made using computer simulations. Correlated Gaussian noise (mean = 0, variance = 2) was used as an input to the main and auxiliary channels of the sidelobe canceler. At the 250th range cell a constant signal at  $S/N = -20$  dB is introduced. The signal residue for both algorithms with canceler

\*B. Widrow, P. E. Mantey, L. J. Griffiths, and B. B. Goode, Proc. IEEE 55, 2143-2159 (1967).

†F. Kretschmer and B. L. Lewis, "An Improved Algorithm for Adaptive Processing," NRL Report 8084, Dec. 1976.

parameters of  $k = 1 - 2\pi$  (0.000124) and  $G = 100$  is shown in Figs. 4 and 5. Although the LMS algorithm had unstable performance, the improved algorithm had completely stable performance. Also, for slow loops there will be ringing in the LMS algorithm, which will result in degraded cancellation performance. In a previous paper Kretschmer\* investigated cascading sidelobe canceler stages as a method of obtaining improved cancellation ratios and transient responses. Thus a higher effective loop gain would be achieved with low actual loop gains, which are required for stable operation. In lieu of their later work, the improved algorithm provides another way of obtaining high loop gains. Lewis and Kretschmer are now working on an open-loop digital implementation of a sidelobe canceler.

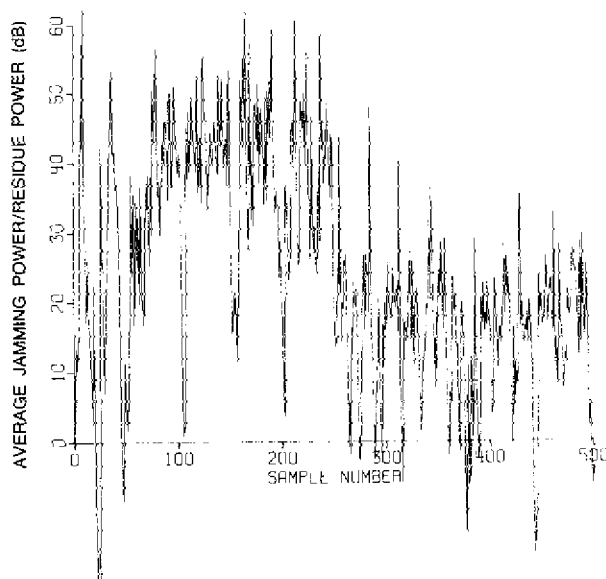


Fig. 4 — Adaptive-canceler response of the LMS algorithm

The sidelobe canceler removes the jamming signal after it has entered the main antenna. Adaptive arrays, which require individual receiving elements, attempt to prevent jamming from entering the antenna receive pattern by placing a receiving antenna null in the direction of the jammer. Before commencing with a discussion of adaptive arrays and radars, it is pointed out that the September 1976 issue of the IEEE Transactions on Antennas and Propagation is a special issue on adaptive arrays and contains many interesting articles.

#### Adaptive Arrays and Radars

Qualitatively, in an adaptive array the received signal is the weighted sum of the signal at the individual receiving elements, with the weights being a function of the received signal. The theory of adaptive arrays was first discussed by Applebaum,<sup>†</sup> and Widrow et al.<sup>‡</sup> have

\*F. F. Kretschmer, IEEE International Radar Conf., 181-185, 1975.

†S. P. Applebaum, "Adaptive arrays," Syracuse University Research Corp. Report SPL-769, June 1964.

‡B. Widrow, P. E. Mantey, L. J. Griffiths, and B. B. Goode, Proc. IEEE 55, 2143-2159 (1967).

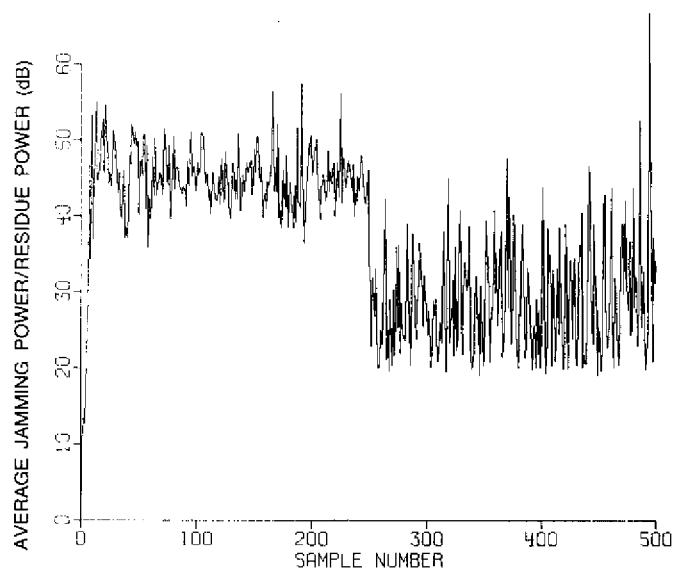


Fig. 5 — Adaptive canceler response of the Kretschmer-Lewis algorithm

made major contributions to the theory; however a later development of Brennan and Reed\* will be followed. Their approach is similar to Applebaum's in that they maximize  $S/N$ , which they show is equivalent to maximizing the probability of detection when the noise is Gaussian distributed.

Let the radar be composed of  $N$  receiving elements, and let the last  $M$  time samples from each element be processed. Thus there are  $n = NM$  space-time samples. Define  $S$  to be a complex (amplitude and phase)  $n$ -vector which contains the desired signal components, and define  $X$  to be a complex  $n$ -vector containing the noise samples. The radar return  $Z$  is given by

$$Z = S + X. \quad (17)$$

To detect the signal  $S$ , the radar output is passed through a linear filter described by a weighting vector  $W$ . Thus the output of the detector (the filter) is

$$Y = W^T Z. \quad (18)$$

Brennan and Reed showed that  $S/N$  at the output of the filter is

$$\left( \frac{S}{N} \right)_o = \frac{|W^T S|^2}{W^T K W}, \quad (19)$$

where the asterisk indicates the complex conjugate and  $K$  is the noise covariance matrix,  $K = E\{X^* X^T\}$ ,  $X$  having zero mean. Consequently what is required is the value of  $W$  that maximizes (19). If the Schwarz inequality is used, it can be shown that the maximum value of (19) is  $S^T K^{-1} S^*$  and that this value is obtained when

$$W = a' K^{-1} S^*, \quad (20)$$

\*L. E. Brennan and I. S. Reed, IEEE Trans. Aerospace and Electronic Systems AES-9, 237-252 (1973).

where  $a'$  is an arbitrary nonzero complex number. This criterion has been known for some time.\* However, it is rarely used, since  $K$  is not known a priori, and if  $K$  is estimated, it has been extremely difficult to invert  $K$  in real time.

What makes the Brennan-and-Reed approach different from other adaptive array processing is not the ability to place spatial nulls in the direction of jammers but rather the temporal processing that is equivalent to a motion-compensated MTI (moving-target indicator). The compensated MTI behavior is obtained by selecting the proper steering signal  $S$ . The selection of the steering signal  $S$  will be illustrated for the case of an airborne coherent pulsed radar.

Assume that the return is range gated, there are  $N_R$  range cells, and the return from the  $j$ th cell is

$$Z(j) = X(j) + S(j). \quad (21)$$

The return signal from the  $r$ th receiving element and  $m$ th time sample can be written as

$$S_r(m) = b_r e^{im\gamma}, \quad r = 1, \dots, N, \quad (22)$$

where  $\gamma = -4\pi VT/\lambda$  is the doppler phase shift, with  $V$  being the relative velocity of the target,  $T$  being the time between transmitted pulses, and  $\lambda$  being the radar wavelength. The quantity  $b_r$  is

$$b_r = A_r e^{i\phi_r + i\delta}, \quad r = 1, \dots, N, \quad (23)$$

where  $A_r$  is the signal amplitude at the  $r$ th element,  $\delta$  is a constant phase factor, and  $\phi_r$  is the relative phase between the target and the  $r$ th element. For a linear array with element spacing  $d$ , the phase angles  $\phi_r$  for a signal arriving at an angle  $\psi$  with respect to the array normal are

$$\phi_r = \frac{2\pi rd}{\lambda} \sin \psi, \quad r = 1, \dots, N. \quad (24)$$

Thus the expected signal for a linear array can be obtained by substituting (23) and (24) into (22).

Both clutter and target will have returns of the form of (22). Since the velocity of the target (and consequently the relative velocity  $V$ ) is unknown, it is impossible to specify  $S$  for the optimal weighting given by (20). However, since (22) is computable for ground clutter as a function of the radar-clutter-cell geometry, one selects a steering signal  $S$  which is orthogonal to the ground-clutter vector  $S'$ . Thus the purpose of  $S$  is to reject the clutter, not to detect the target. This is about as close to an optimal detector as one can obtain, since it can be shown\* that no uniform most-powerful test exists when the target velocity is unknown.

As an example let  $M = 2$  and assume one wants to detect a target in a direction normal to the direction of the platform velocity (the radar is sidelooking). Then  $S_r(m) = A_r e^{i\delta}$ , and for uniform amplitude taper ( $A_r = 1, r = 1, \dots, N$ ) the clutter signal is

$$S'^T = e^{i\delta} [1, \dots, 1, 1, \dots, 1]. \quad (25)$$

The appropriate steering signal  $S$  which is orthogonal to  $S'$ ,  $S'^T S'^* = 0$ , is

$$S^T = [1, \dots, 1, -1, \dots, -1], \quad (26)$$

\*H. L. VanTrees, IEEE Trans. Military Electronics MIL-9, 216-229 (1965).

which corresponds to a target at 1/2 the blind speed of the radar:

$$V = \frac{1}{2} \left[ \frac{\lambda}{2T} \right]. \quad (27)$$

Thus, if (26) is used in (20), the detector is optimized for canceling main-beam clutter. We now consider how (20) can be implemented adaptively.

Brennan and Reed use the method of steepest ascent to maximize S/N:

$$F \triangleq \frac{|W^T S|^2}{W^{T*} K W}. \quad (28)$$

The recursive algorithm for steepest ascent is

$$W(j+1) = W(j) + \frac{1}{2} \mu(j) \nabla F[W(j)], \quad (29)$$

where  $\nabla F[W(j)]$  is the complex gradient of  $F$  evaluated at  $W(j)$ , which has been shown to be

$$\nabla F = 2 \left[ \frac{W^T S}{W^{T*} K W} \right] \left[ S^* - \left[ \frac{W^T S^*}{W^{T*} K W} \right] K W \right]. \quad (30)$$

If  $K$  is assumed known and  $\mu(j)$  is chosen to be a constant, one can apply known theorems\* to show  $W(j)$  approaches a critical point as a limit. Thus, if  $W(0)$  is sufficiently close to the optimal value,  $W(j)$  approaches  $a'K^{-1}S^*$  in the limit.

The trouble with using (30) in (29) is that  $\nabla F$  is a nonlinear function of  $W(j)$ , which in some adaptive systems can cause computational difficulties. Hence the algorithm was linearized by noting

$$\lim_{j \rightarrow \infty} \frac{W^T S}{W^{T*} K W} = \frac{1}{a'} \triangleq a. \quad (31)$$

Thus, if  $\mu(j)$  equals a constant  $\mu$ , (29) reduces to

$$W(j+1) = W(j) + \mu a [S^* - a^* K(j) W(j)], \quad (32)$$

where  $K(j)$  is a statistical estimate of the unknown covariance matrix  $K$ . The best (maximum-likelihood) estimate of  $K$  is

$$K(j) = Z^*(j) Z^T(j). \quad (33)$$

Brennan and Reed then showed that (32) converged. Specifically, the expected value of (32) converges to  $a' \bar{K}^{-1} S^*$ , where  $\bar{K} = E\{K(j)\}$  for all  $j$ , if  $Z(j)$  are independent and  $0 < \mu < 2a'^2 / \max \lambda_i$ , where  $\lambda_i$  ( $i = 1, \dots, n$ ) are the eigenvalues of  $\bar{K}$ .

The block diagram of the adaptive radar is shown in Fig. 6, and the implementation of an adaptive loop is shown in Fig. 7. The steady-state antenna pattern can be calculated from (20), and the S/N improvement can be found from  $S^T K^{-1} S^*$ . However in many radar environments the clutter has a temporal and spatial variation; consequently the rate of convergence is important. To study this phenomena, computer simulations were used.

\*M. J. D. Powell, SIAM Rev. 12, 79-97 (1970).

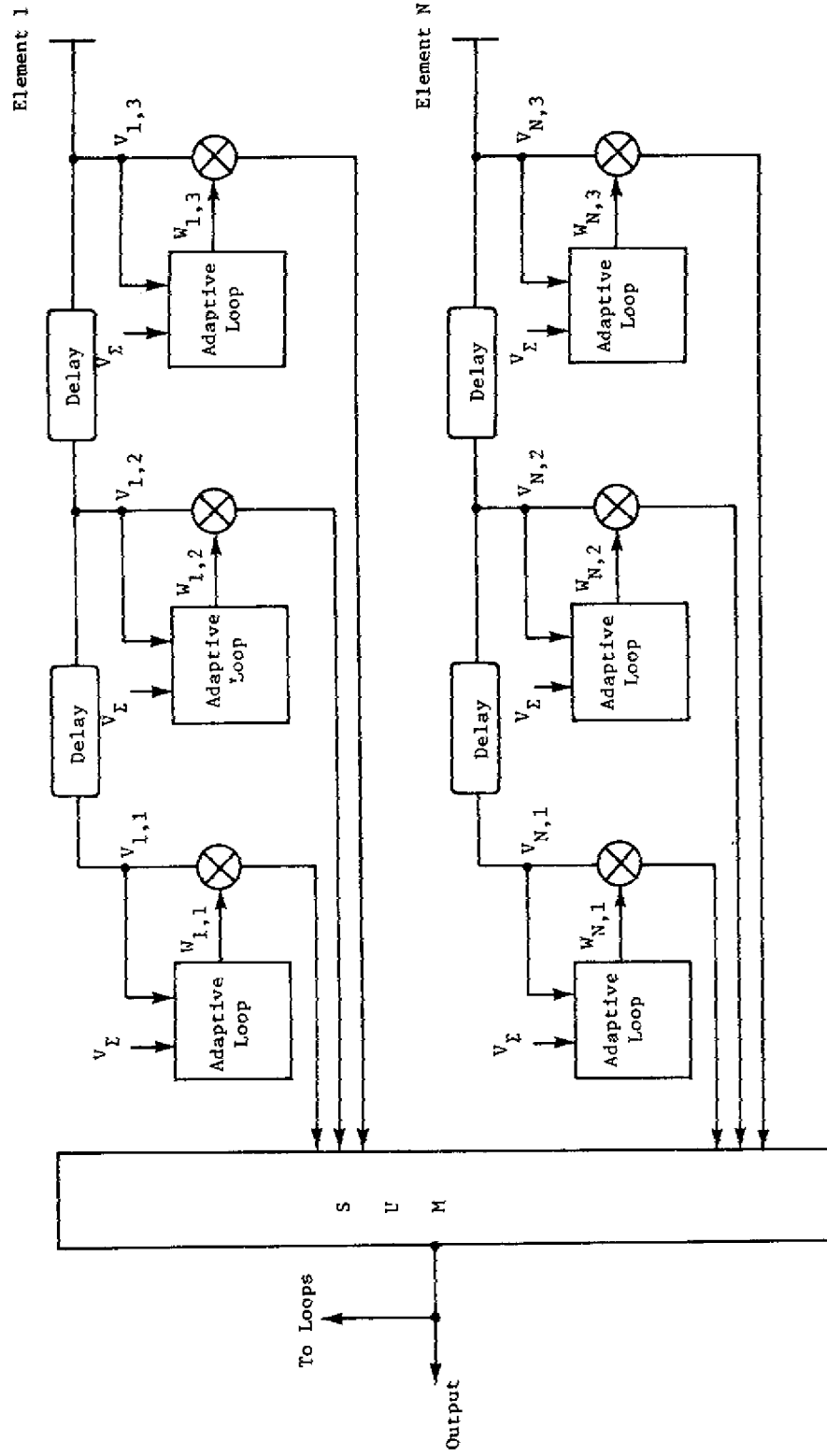


Fig. 6 — Adaptive AMTI radar using control loops. (From L. E. Brennan, J. D. Mallett, and I. S. Reed, IEEE Trans. Antennas and Propagation AP-24, 607-615 (1976), courtesy of the Institute of Electrical and Electronics Engineers.)

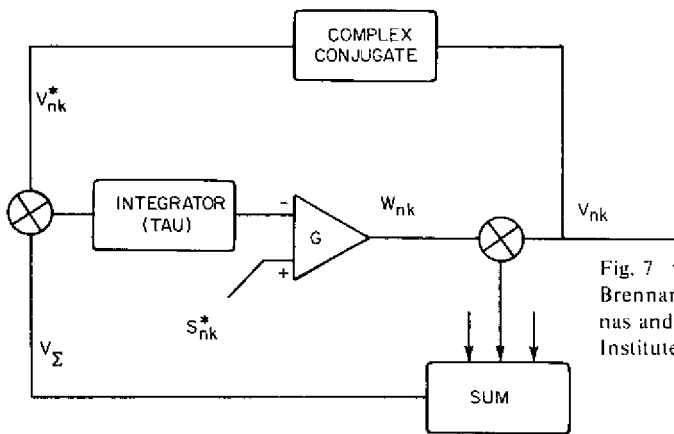


Fig. 7 — Implementation of an adaptive loop. (From L. E. Brennan, J. D. Mallett, and I. S. Reed, IEEE Trans. Antennas and Propagation AP-24, 607-615 (1976), courtesy of the Institute of Electrical and Electronics Engineers.)

The basic parameters for a ten-element adaptive array using only one time sample ( $N = 10$  and  $M = 1$ ) are given in Table 1. In the first simulation, 30 discrete clutter points were uniformly distributed in the two symmetrical intervals  $[17^\circ, 90^\circ]$  and  $[-17^\circ, -90^\circ]$ , and the radar was looking normal to the aircraft velocity vector. The simulation results are summarized in Fig. 8, where the base of the plot is 45 dB below the peak gain. The back antenna pattern is the initial receiving pattern, the middle eight patterns are from range cells 200 to 1600 in 200 range-cell intervals, and the last pattern is the steady-state pattern. Since there are 30 interference sources and only 10 elements, it is impossible to put a null at each interference angle. Rather the adaptive array follows two strategies: it widens the main beam and consequently lowers the general sidelobe level, and it places receiver nulls at transmitter maximums and vice versa. After 1600 interactions all but 1.6 dB ( $27.3 - 25.7$ ) of the maximum signal-to-clutter improvement has been obtained.

In the second simulation the 30 clutter points were placed nonsymmetrically about zero in the interval  $[15^\circ, 45^\circ]$ . The simulation results are summarized in Fig. 9. Although the sidelobes are reduced in the proper angular interval, after 1600 iterations only 24.7 dB of the possible 44.1-dB improvement in the signal-to-clutter ratio has been obtained. Brennan and Reed have shown that the time behavior of the weights is a sum of exponentials of the form

$$W_i = \sum_{l=1}^N C_{il} e^{[-(G\lambda_l + 1)t/\tau]}, \quad (34)$$

where  $\tau$  is the time constant and  $G$  is the gain of the low-pass filter. Thus the rate of convergence is controlled by the smallest eigenvalue of  $K$ ; specifically, the effective time constant is  $\tau/(G\lambda_{\min} + 1)$ . This suggests that rapid convergence can be obtained by selecting  $G$  to be large and/or  $\tau$  to be small. However this is not a useful solution to the convergence problem, since Brennan et al.\* have shown that the total output noise power in the adaptive array is

$$P = \mathbf{W}^T \mathbf{K} \mathbf{W} \left[ 1 + \frac{G}{2\tau} \sum_{l=1}^N \lambda_l \right], \quad (35)$$

\*L. E. Brennan, E. L. Pugh, and I. S. Reed, IEEE Trans. Aerospace and Electronic Systems AES-7, 254-262 (1971).

Table 1 — Parameters Assumed in a  
Simulation of an Adaptive Receiving Array

Ten-element linear array  
 Element patterns isotropic over  $-\pi/2 \geq \nu \leq \pi/2$   
 Half-wave-spaced elements  
 Uniformly illuminated transmit array  
 30 scatterers in the sidelobe region, equally spaced in angle  
 No interference for  $-\theta_1 < \theta < \theta_1$   
 Each receiving-element weight controlled adaptively  
 Simulation of 1600 independent sets of input signals (range  
 resolution cells)  
 No receiver noise

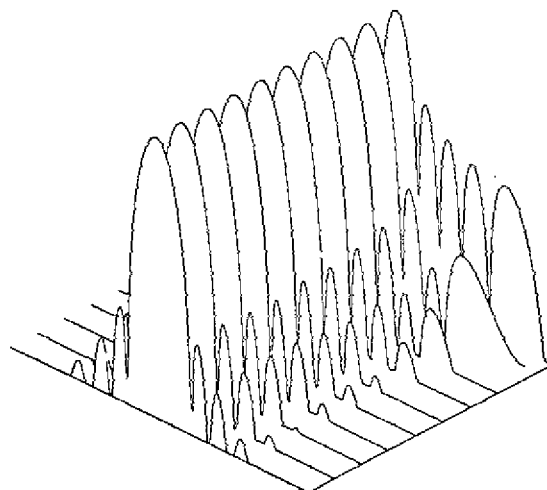
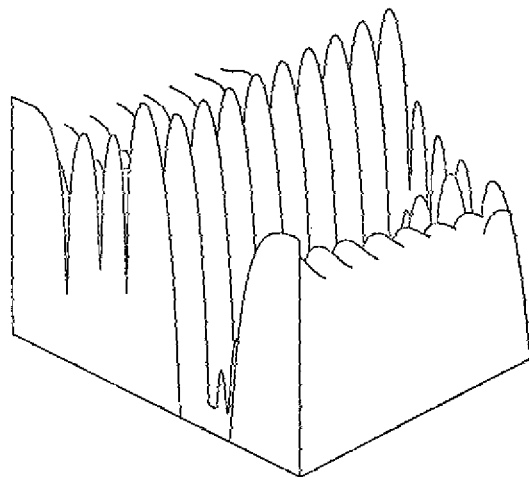


Fig. 8 — Projectograph plot of the gain of a ten-element adaptive array in the case of symmetric clutter distribution. The improvement in the signal-to-sidelobe clutter ratio from the initial receiving pattern (at the rear) is 27.3 dB for steady state (pattern at the front) and 25.7 dB after 1600 iterations. (From L. E. Brennan and L. S. Reed, IEEE Trans. Aerospace and Electronic Systems AES-9, 237-252 (1973), courtesy of the Institute of Electrical and Electronics Engineers.)

Fig. 9 — Projectograph plot of the gain of a ten-element adaptable array in the case of nonsymmetric clutter distribution. The improvement in the signal-to-sidelobe clutter ratio is 44.1 dB for steady state (not shown) and 24.7 dB after 1600 iterations (pattern at the front). (From L. E. Brennan and L. S. Reed, IEEE Trans. Aerospace and Electronic Systems AES-9, 237-252 (1973), courtesy of the Institute of Electrical Engineers.)



where  $\mathbf{W}$  is the average weight vector in the absence of loop noise (departure from steady state). The quantity  $\mathbf{W}^T \mathbf{K} \mathbf{W}$  is the noise power when  $\mathbf{W} = \mathbf{K}^{-1} \mathbf{S}^*$ . Consequently, the output power has been increased by the factor  $G \Sigma \lambda_j / 2\tau$  due to loop noise. Thus, when  $\mathbf{K}$  contains both small and large eigenvalues, it is impossible to select a  $G$  and  $\tau$  which yield both rapid convergence and low loop noise. To avoid the convergence problem, Reed et al.\* have suggested a direct computation of the weights.

The maximum-likelihood estimate of  $\mathbf{K}$ , assuming the noise is Gaussian distributed, is

$$\hat{\mathbf{K}} = \frac{1}{L} \sum_{j=1}^L \mathbf{Z}^*(j) \mathbf{Z}^T(j). \quad (36)$$

Since  $\mathbf{Z}^*(j) \mathbf{Z}^T(j)$  is an  $n$ -by- $n$  matrix of rank 1,  $L$  must be  $\geq n$  for the inverse to exist. Then the filter has the form

$$\hat{\mathbf{W}} = \hat{\mathbf{K}}^{-1} \mathbf{S}^*. \quad (37)$$

The output S/N for (37) normalized by the maximum S/N,  $\mathbf{S}^T \mathbf{K}^{-1} \mathbf{S}^*$ , which corresponds to (20), is

$$\rho(\hat{\mathbf{K}}) = \frac{(\mathbf{S}^T \hat{\mathbf{K}}^{-1} \mathbf{S}^*)^2}{(\mathbf{S}^T \mathbf{K}^{-1} \mathbf{S}^*) (\mathbf{S}^T \hat{\mathbf{K}}^{-1} \mathbf{K} \hat{\mathbf{K}}^{-1} \mathbf{S}^*)}. \quad (38)$$

The expected value of (38) is

$$E\{\rho(\hat{\mathbf{K}})\} = (L + 2 - n) / (L + 1). \quad (39)$$

Thus the average loss can be kept less than 3 dB ( $E\{\rho(\hat{\mathbf{K}})\} \geq 1/2$ ) by letting  $L \geq 2n$ .

However, whereas the adaptive loops of Fig. 6 require  $n$  complex multiplications, the sample-matrix inverse method requires approximately  $n^3$  complex multiplications. To reduce the complexity of the method, one can update the covariance matrix using

$$\hat{\mathbf{K}}_j = (1 - \alpha) \hat{\mathbf{K}}_{j-1} + \alpha \mathbf{Z}^*(j) \mathbf{Z}^T(j), \quad (40)$$

where  $\alpha$  is the weight applied to the current sample. Then the inverse of  $\hat{\mathbf{K}}_j$ , given  $\hat{\mathbf{K}}_{j-1}$ , is†

$$\hat{\mathbf{K}}_j^{-1} = \frac{\hat{\mathbf{K}}_{j-1}^{-1}}{1 - \alpha} - \left( \frac{\alpha}{1 - \alpha} \right) \frac{\left[ \hat{\mathbf{K}}_{j-1}^{-1} \mathbf{Z}^*(j) \right] \left[ \mathbf{Z}^T(j) \hat{\mathbf{K}}_{j-1}^{-1} \right]}{(1 - \alpha) + \alpha \mathbf{Z}^T(j) \hat{\mathbf{K}}_{j-1}^{-1} \mathbf{Z}^*(j)}. \quad (41)$$

This method of updating the inverse requires approximately  $2n^2$  complex multiplications. The average computation time for updating the weights  $\mathbf{W}$  depends on how frequently they must be updated. For example, depending on the radar environment, updating the weights every PRF using (36) may be quite adequate; consequently the computation time may be less than that of the adaptive loops.

Brennan et al.‡ compared the convergent rates of the three methods using a computer simulation illustrating airborne MTI performance. The results of the simulation are shown in

\*I. S. Reed, J. D. Mallett, and L. E. Brennan, IEEE Trans. Aerospace and Electronics Systems AES-10, 853-863 (1974).

†J. M. Shapard, D. Edelblute, and G. Kinnison, Naval Undersea Research and Development Center Report NUC-TN-528, May 1971.

‡L. E. Brennan, J. D. Mallett, and I. S. Reed, IEEE Trans. Antennas and Propagation AES-24, 607-615 (1976).

Fig. 10. In both instances, (a) forward looking and (b) sidelooking, the two methods of calculating  $\hat{K}^{-1}$  provide an excellent convergent rate. Figure 10 indicates an MTI gain of plus 100 dB, but in practice the MTI gain would be limited to a lower figure by internal clutter motion.

Most work on adaptive arrays and radars has been limited to theoretical studies. However there has been some experimental work at Ohio State University,\* the Naval Research Laboratory,† and the Wide-Aperture HF Radio Research Facility operated by Stanford Research Institute.‡§

### Moving-Target Indicators

Moving-Target Indicators (MTIs) were first investigated in the 1940's, and they have been discussed in detail in the books by Skolnik#\*\* and Nathanson††. The coherent MTI, the most common MTI, uses an internal coherent reference source to distinguish a moving target from fixed clutter returns. The MTI signal is obtained by coherently subtracting the returned voltages from successive transmitted pulses:

$$Z'_i(j) = Z_i(j) - Z_{i-1}(j), \quad (42)$$

where  $Z_i(j)$  is the  $i$ th returned pulse in the  $j$ th range cell. Larger clutter attenuations can be obtained by using multiple pulses. The frequency (doppler) response of the MTI is that of a bandpass filter.

The most serious problems associated with MTI are limiting and blind speeds. The first of these can be covered very simply. In the classic paper of Ward and Shrader‡‡ it was shown that MTI improvement could be degraded by 20 dB in a three-pulse canceler by limiting the clutter return. Their work showed that the degradation was fundamental to limiting and that consequently a large dynamic range is required to avoid limiting.

The major problem with MTI is that blind speeds, corresponding to doppler frequencies higher than Nyquist rate, occur at

$$V_B = \frac{\ell\lambda}{2T}, \quad \ell = 1, 2, 3, \dots \quad (43)$$

Thus for an L-band (1.3-GHz) radar with a PRF of 300 pps the blind speeds occur at multiples of approximately 70 knots. Because of the width of the clutter notch (rejection region of the canceler), many air targets would not be detected. There are several solutions to the problem

\*R. T. Compton, IEEE Trans. Antennas and Propagation AP-24, 697-706 (1976).

†W. F. Gabriel, "Proceedings Adaptive Antenna Systems Workshop March 11-13, Vol. 1", NRL Report 7803, Sept. 1974.

‡L. J. Griffiths, IEEE Trans. Antennas and Propagation AP-24, 707-720 (1976).

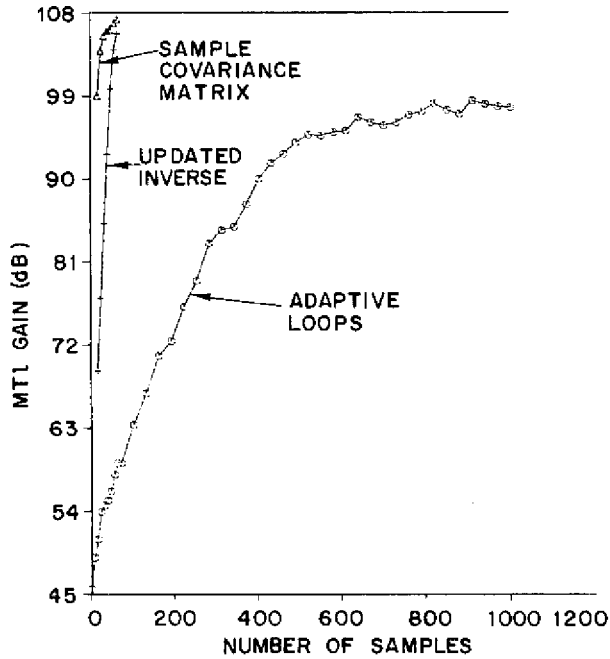
§T. W. Washburn and L. E. Sweeney, Jr., IEEE Trans. Antennas and Propagation AP-24, 721-732 (1976).

#M. I. Skolnik, *Introduction to Radar Systems*, McGraw-Hill, New York, 1962.

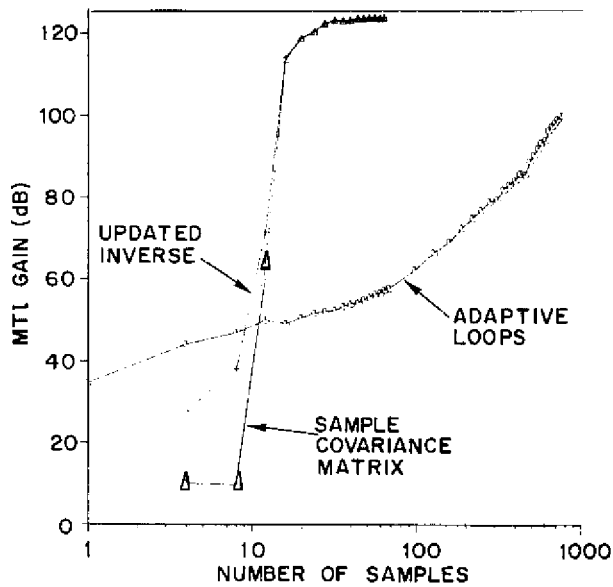
\*\*M. I. Skolnik, editor *Radar Handbook*, McGraw-Hill, New York, 1970.

††F. E. Nathanson, *Radar Design Principles*, McGraw-Hill, New York, 1969.

‡‡H. R. Ward and W. W. Shrader, EASCON Convention Record, 168-173, 1968.



(a) Scan angle = 0.0° and steady-state gain = 108.1 dB



(b) Scan angle = 90.0° and steady-state gain = 125.5 dB

Fig. 10 — Adaptive performance as a function of the number of samples (eight elements, two pulses, element spacing = 0.5, interpulse motion = 0.2). (From L. E. Brennan, J. D. Mallett, and I. S. Reed, *IEEE Trans. Antennas and Propagation AP-24*, 607-615 (1976), courtesy of the Institute of Electrical and Electronics Engineers.)

of blind speeds in MTIs. Among these are variable PRF, staggered-PRF MTI, and dual-frequency MTI.

The simplest solution is to use a variable-PRF system. If an interpulse period of  $T$  is used, a blind speed of  $V_B$  is obtained. Then, if the interpulse period is changed by a small fraction  $r$ , the blind speed changes by the same fraction  $r$ , and the smallest common blind speed is  $V_B/(1 - r)$ . Thus, if an L-band radar has two PRFs, 300 pps and 270 pps, the blind speed of the radar system is approximately 700 knots. There are two disadvantages of such a system: (a) second-time-around clutter (clutter beyond the unambiguous range, caused by ducting at sea or high-altitude long-range clutter such as mountains and chaff) passes through the MTI, and (b) the constant PRF for a two- or three-pulse burst makes the system more vulnerable to jamming. The simple solution to (a), using an extra filler pulse (transmitting three pulses but only using the last pulse out of a two-pulse MTI), makes situation (b) worse.

An elegant solution to the blind-speed problem is the staggered-PRF MTI. The basic MTI configuration is shown in Fig. 11. The interpulse durations  $\tau_i$  are constrained by the relation

$$F_B \tau_i = \ell_i, \quad (44)$$

where  $F_B$  is the first blind doppler frequency and  $\ell_i$  are integers for all  $i$ . Capon\* showed that the optimal weights  $\{a_i\}$  for minimizing the output clutter residue while retaining some fraction of the average gain of the filter (this constraint avoids the trivial solution  $a_i = 0$ , for all  $i$ ) are the components of the eigenvector associated with the smallest eigenvalue of the clutter covariance matrix. This procedure ignores what happens in the filter passband. Hsiao and Kretschmer† developed a procedure for setting the interpulse periods to minimize the RMS passband ripple while maintaining the minimum clutter residue. A typical response is shown in Fig. 12. The basic trouble with this system is that second-time-around clutter will not be canceled.

A third solution to the blind-speed problem is the dual-frequency MTI first discussed by Kroszczyński‡§ and later by Hsiao#. The system works by transmitting two frequencies whose ratio  $r$  is slightly less than 1, filtering out the sum signal and retaining the difference signal. The system performance is basically that of a low-frequency radar; hence the blind-speed problem is reduced. The detrimental factor is that the clutter improvement factor is reduced by several dB. A typical filter response for a dual-frequency MTI is shown in Fig. 13. Although the passband response is quite variable, no attempt has been made to reduce the variation by changing  $r$ . Hsiao indicates that the staggered-PRF MTI is preferable to the dual-frequency MTI. However this author believes that the dual-frequency MTI should not be discarded that readily. An alternate solution, and possibly a better one, is to operate individual MTIs at the two frequencies.

\*J. Capon, IEEE Trans. Information Theory **IT-10**, 152-159 (1964).

†J. K. Hsiao and F. F. Kretschmer, Jr., The Radio and Electronic Engineer **43**, 689-693 (1973).

‡J. Kroszczyński, Radio and Electronic Engineer **34**, 157-159 (1967).

§J. Kroszczyński, Radio and Electronic Engineer **39**, 172-176 (1970).

#J. K. Hsiao, The Radio and Electronic Engineer **45**, 351-356 (1975).

Fig. 11 — A staggered-PRF MTI filter.  
 (From J. K. Hsiao and F. F. Kretschmer, *Radio and Electronic Engineer* 43, 689-693 (1973), courtesy of the Institution of Electronic and Radio Engineers.)

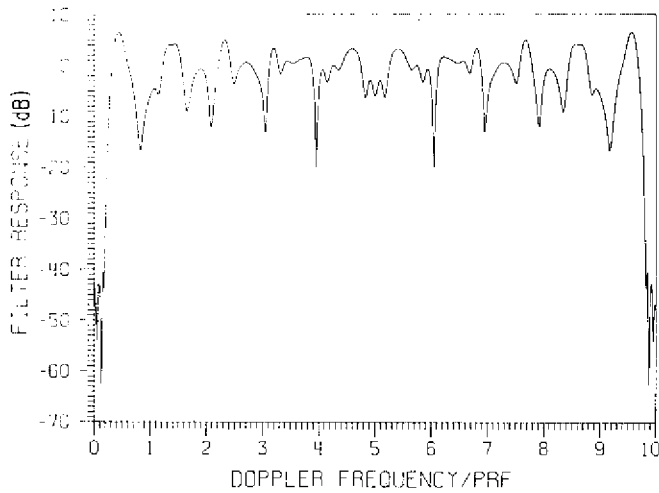
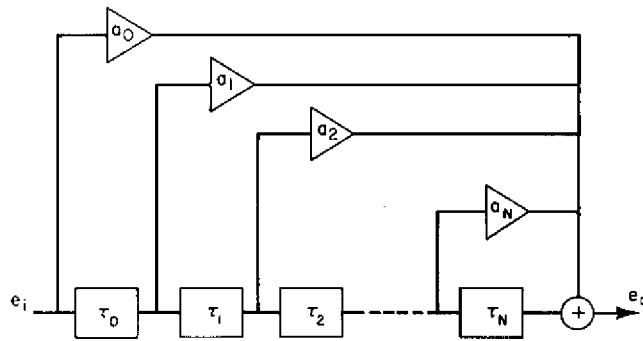
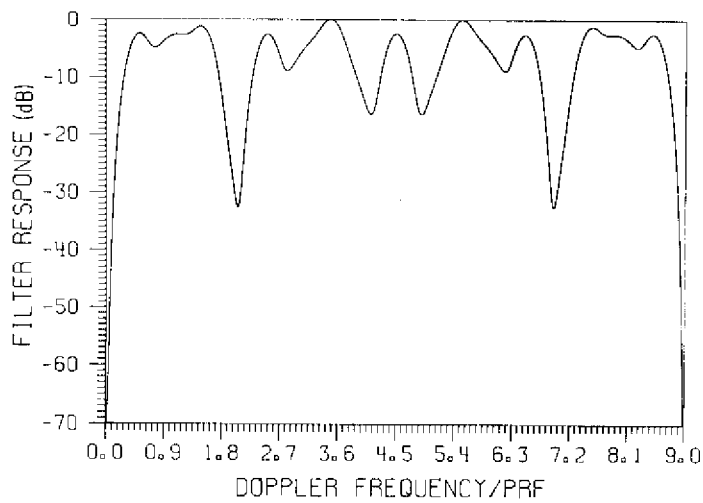


Fig. 12 — Frequency response for a seven-pulse staggered-PRF MTI filter.  
 (From Hsiao and Kretschmer, *Radio and Electronic Engineer* 43, 689-693 (1973), courtesy of the Institution of Electronic and Radio Engineers.)

Fig. 13 — Target-signal gain function of a dual-frequency MTI system with  $r = 0.89$ .  
 (From J. K. Hsiao, *Radio and Electronic Engineer* 45, 351-356 (1975), courtesy of the Institution of Electronic and Radio Engineers.)



## Doppler Processing

An MTI canceler provides near optimal target detection in clutter but provides little or no improvement against receiver noise. McAulay\* formulated the problem as a classical detection problem and showed that the optimal detector could be structured approximately as an MTI canceler followed by a narrow-band doppler filter bank. This structure has the practical advantage of greatly reducing the dynamic range required at the input of the filter bank. In this configuration, the MTI canceler provides improvement against clutter, and the doppler filter bank provides improvement against noise.

The moving-target detector (MTD), developed by Lincoln Laboratory†† for the FAA, uses this type of processing. During 1976 the MTD was tested with a modified FPS-18 radar at the FAA facility in Atlantic City, N.J. The modified FPS-18 radar is an S-band radar instrumented to 48 n.mi. The range cell is approximately 1/16 n.mi., the beamwidth is 1.5°, the scan rate is 15 rpm, and 20 pulses are returned as the radar sweeps past the target.

A block diagram of the MTD signal processor is shown in Fig. 14. An azimuth cell is defined as a half beamwidth (0.75°) and contains ten pulses, with the time lapse for the ten pulses being referred to as a coherent processing interval (CPI). In a CPI the ten pulses are passed through a three-pulse MTI canceler, and the eight output pulses (two pulses are needed to load the MTI) serve as an input to an eight-point FFT, the points being weighted to provide low filter sidelobes. The radar PRF is changed from 1000 pps to 1150 pps on alternate CPIs to avoid the blind-speed problem.

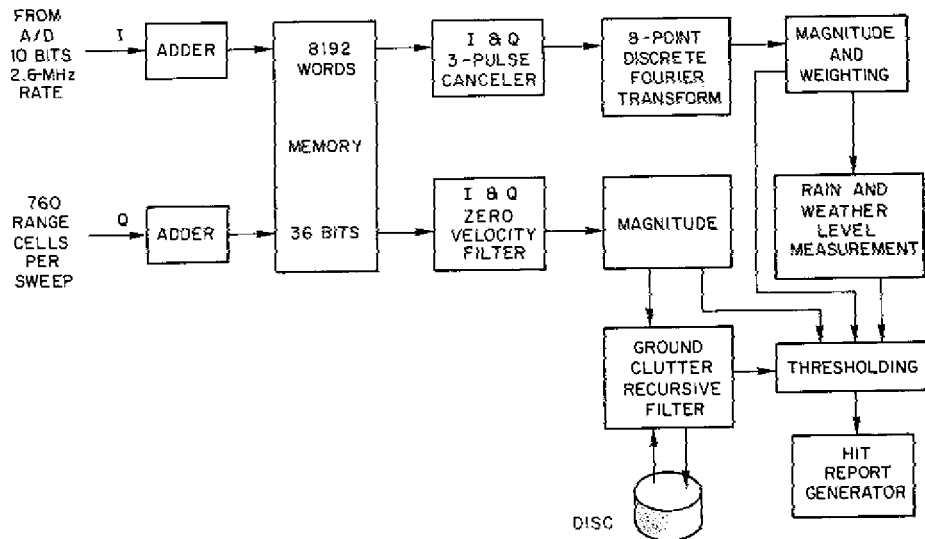


Fig. 14 — MTD signal processor

\*R. J. McAulay, Tech. Note 1972-14, Lincoln Laboratory, Mass. Inst. of Tech., 1972

†R. M. O'Donnell, C. E. Muehe, M. Labitt, W. H. Drury, and L. Cartledge, EASCON Convention Record 71-75, 1974

‡C. E. Muehe, L. Cartledge, W. H. Drury, E. M. Hofstetter, M. Labitt, P. B. McCorsion, and V. J. Sferriano, Proc. IEEE 62, 716-723, (1974).

The  $2.9 \times 10^6$  range-azimuth-doppler cells ( $760 \times 360/0.75 \times 8$ ) are individually thresholded. In this process a clutter map is generated by weighting the radar return in the zero-doppler filter over the last eight scans (32 s) using a digital filter. Thus tangential targets having zero doppler can be detected if the target level exceeds the clutter-map level by a specified constant. That is, tangential targets can be detected in spotty ground clutter by using the principle of interclutter visibility\*. The thresholds for filters 2 through 6 are set using a mean-level threshold. Specifically the threshold for a given-number filter is based† on the average return in the given-number filter from the range cells  $\leq 1/2$  n.mi. (eight cells) on either side of the test cell. Since clutter spills over into filters 1 and 7, two thresholds are generated for these filters. One threshold is based on the map, a second threshold is based on the mean level over a range interval, and the higher of the two thresholds is used.

The MTD represents a great improvement in signal processing for FAA air-surveillance radars. A good match of processor to radar has been designed, and component technology has made the processing practical to implement. Presently, a second-generation MTD is being designed. This MTD uses no MTI, but rather each filter is optimized to obtain the maximum signal-to-clutter-plus-noise ratio for an assumed clutter spectrum.

### Noncoherent Moving-Target Indicators

Noncoherent MTIs are described in Skolnik's *Introduction to Radar Systems*‡ and *Radar Handbook*.§ They differ from coherent MTI by not using an internal coherent reference source but rather mixing the received signal with itself. Thus, when both clutter and a target are present, the beat between them yields a return at the target doppler. On the other hand, when only a target is present, the signal return is at zero doppler and cannot be detected. Consequently, for noncoherent MTI to be useful, gating circuitry is required for passing the noncoherent MTI output when clutter is present and passing the regular video when clutter is not present. Generally fringe areas cause major problems for the gating circuitry, making performance unacceptable.

A different kind of noncoherent MTI has been made possible by high-power microwave sources.# Lewis and Cantrell\*\* propose transmitting a short pulse and subtracting successive noncoherent pulses. This is similar to an area MTI discussed in *Introduction to Radar Systems*,‡ except that the short pulse enables the subtraction to be made on a pulse-to-scan pulse rather than a scan-to-scan basis. Thus, with a 1 ns pulse and a PRF of 200 pps, all moving targets above 60 knots can be detected; that is, there are no blind speeds.

\*D. K. Barton and W. W. Shrader, EASCON Conv. Record 294-297, 1969.

†Details about various thresholding techniques can be found in the section on noncoherent processing

‡M. I. Skolnik, *Introduction to Radar Systems*, McGraw-Hill, New York, 1962.

§M. I. Skolnik, editor *Radar Handbook*, McGraw-Hill, New York, 1970.

#V. L. Granatstein, P. Sprangle, M. Herndon, R. K. Parker, and S. P. Schlesinger, *J. Applied Physics* **46**, 3800-3805 (1975).

\*\*B. L. Lewis and B. H. Cantrell, "Short Pulse Noncoherent MTI", patent application, Navy Case 60372, NRL, Nov. 1975.

## NONCOHERENT DETECTION

The earliest noncoherent signal processing was performed by radar operators using visual inputs from PPIs and A-scopes. Although operators can perform this detection task accurately, operators are easily saturated and become quickly fatigued. To remedy this situation and to provide quick reaction times, automatic detection and tracking (ADT) systems have become quite popular during the 1970s. The statistical framework necessary for the development of ADT was introduced to the radar community in the 1940s by Marcum\*, and later Swerling† extended the work to fluctuating targets. They investigated many of the statistical problems associated with the noncoherent detection of targets in Rayleigh noise. Their most important result was the generation of curves of probability of detection ( $P_D$ ) versus signal-to-noise ratio (S/N) for a detector which sums  $N$  enveloped detected samples (either linear or square law) under the assumption of equal signal amplitudes. However, in a search radar, as the beam sweeps over the target, the returned signal amplitude is modulated by the antenna pattern. Many authors investigated various detectors (weightings), comparing detection performance and angular estimation results to the optimal values. The detectors investigated included the moving window, feedback integrator, two-pole filter, binary integrator, and batch processor.

In the original work on these detectors, the environment was assumed known and homogeneous, so that fixed thresholds could be used. However a realistic environment, containing land, sea, and rain for example, will cause an exorbitant number of false alarms for a fixed threshold system. Two approaches, adaptive thresholding and nonparametric detectors, have been used to solve the false-alarm problem. Both solutions are based on the assumption that homogeneity exists in a small region about the range cell that is being tested. The adaptive thresholding method assumes that the noise density is known except for a few unknown parameters. The surrounding reference cells are then used to estimate the unknown parameters, and a threshold based on the estimated density is obtained. Nonparametric detectors obtain a constant false-alarm rate (CFAR) by ranking the test sample with the reference cells. Under the hypothesis that all the samples (test and reference) are independent samples from an unknown density function, the test sample has a uniform density function; consequently a threshold which yields CFAR can be set.

### Classical Theory

The radar detection problem is a binary-hypothesis-testing problem:

$H_0$ : no target present

or

$H_1$ : target present.

Many criteria can be used to solve this problem, but the most appropriate for radar is the Neyman-Pearson‡ criterion. This criterion maximizes  $P_D$  for a given probability of false alarm

\*J. I. Marcum, IRE Trans. Information Theory 6, 59-267 (1960).

†P. Swerling, IRE Trans. Information Theory 6, 269-308 (1960).

‡J. Neyman and E. S. Pearson, Biometrika 20A, 175-240, 263-294 (1928).

( $P_{fa}$ ) by comparing the likelihood ratio ( $L$ ) to an appropriate threshold  $T$ . A target is declared present if

$$L(x_1, \dots, x_n) = \frac{p(x_1, \dots, x_n | H_1)}{p(x_1, \dots, x_n | H_0)} \geq T, \quad (45)$$

where  $p(x_1, \dots, x_n | H_1)$  and  $p(x_1, \dots, x_n | H_0)$  are the joint densities of the  $n$  samples under the conditions of target presence and target absence respectively. For a linear envelope detector and white Gaussian noise the samples have a Rayleigh density under  $H_0$  and a Ricean density under  $H_1$ , and the likelihood detector reduces to

$$\prod_{i=1}^n I_0 \left( \frac{A_i x_i}{\sigma^2} \right) \geq T, \quad (46)$$

where  $I_0$  is the Bessel function of zero order. For equal-amplitude ( $A_i = A$ ) small signal pulses ( $A_i \ll \sigma$ ), the detector reduces to the square-law detector:

$$\sum_{i=1}^n x_i^2 \geq T. \quad (47)$$

This detector and the linear detector were first studied by Marcum\* and were studied in succeeding years by numerous people. The most important facts concerning these detectors are the following:

- The detection performances of the linear and square-law detectors are similar and are close to the performance of the optimal detector.\*
- Since the signal return of a scanning radar is modulated by the antenna pattern, only 0.84 of the pulses between the half-power points should be integrated, and the antenna beam-shape factor (ABSF) is 1.6 dB.† The ABSF is the number by which the midbeam S/N must be reduced so that the detection curves generated for equal signal amplitudes can be used for the scanning radar.
- The collapsing loss for the linear integrator can be much greater than the loss for a square-law integrator.‡ The collapsing loss is the additional signal required to maintain the same  $P_D$  and  $P_{fa}$  when unwanted noise samples along with the desired signal-plus-noise samples are integrated.

Most signal processors are required not only to detect targets but to make angular estimates of the azimuth position of the target. Swerling§ calculated the standard deviation of the optimal estimate by using the Cramer-Rao lower bound. The results are shown in Fig. 15, where a normalized standard deviation is plotted against S/N per pulse. This result holds for a moderate or large number of pulses integrated, and the optimal estimate involves finding the location where the correlation of the returned signal and the derivative of the antenna pattern is zero. Although this estimate is rarely implemented, its performance is approached by simple

\*J. I. Marcum, IRE Trans. Information Theory 6, 59-267 (1960).

†L. V. Blake, Proc. IRE 41, 770-774 (1953).

‡G. V. Trunk, Proc. IEEE 60, 743-744 (1972).

§P. Swerling, Proc. IRE 44, 1146-1155 (1956).

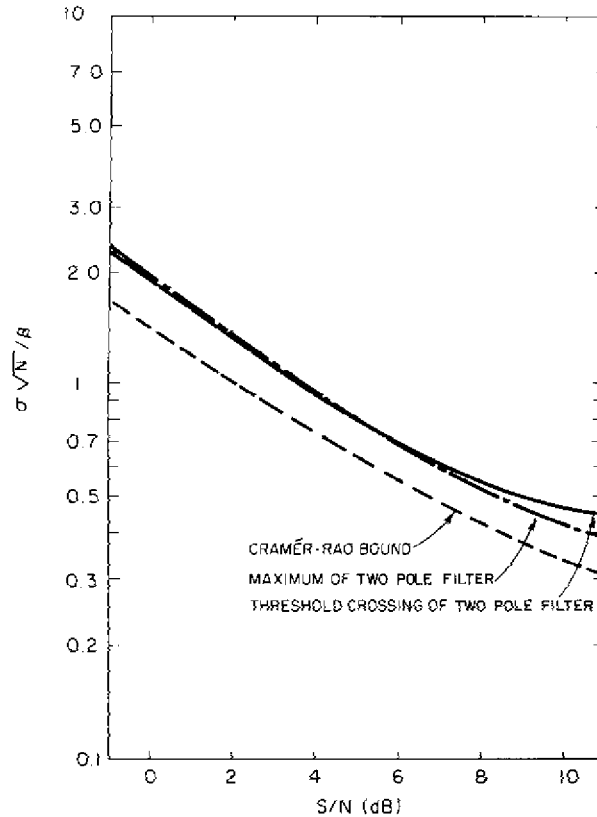


Fig. 15 — Comparison of angular estimates with the Cramer-Rao lower bound. In the ordinate expression,  $\sigma$  is the standard deviation of the estimation error and  $N$  is the number of pulses within the 3-dB beamwidth, which is  $2\beta$ .

estimates, such as the maximum-value and threshold-crossing procedures, as can be seen in Fig. 15.

### Integrators

Almost all signal processors use linear rather than square-law detectors, since a linear detector is easily built by using a matched filter and a half-wave rectifier followed by a low-pass filter. However many different integrators are used to accumulate the linear-envelope-detected pulses. A few of the most common integrators are shown in Fig. 16. Some advantages and disadvantages of these integrators are as follows.\*†‡

#### *Moving window*

The moving window performs a running sum of  $N$  pulses; as the latest pulse is added to the sum, the pulse that is  $N$  PRFs in the past is subtracted from the sum. The detection performance of this detector is only 0.5 dB worse than the optimal detector which weights the returned signal by the fourth power of the voltage antenna pattern. The angular estimate is ob-

\*D. S. Palmer and D. C. Cooper, IEEE Trans. Information Theory **IT-10**, 296-302 (1964).

†G. M. Dillard, IEEE Trans. Information Theory **IT-13**, 2-6 (1967).

‡B. H. Cantrell and G. V. Trunk, IEEE Trans. Aerospace and Electronic Systems **AES-9**, 649-653 (1973).

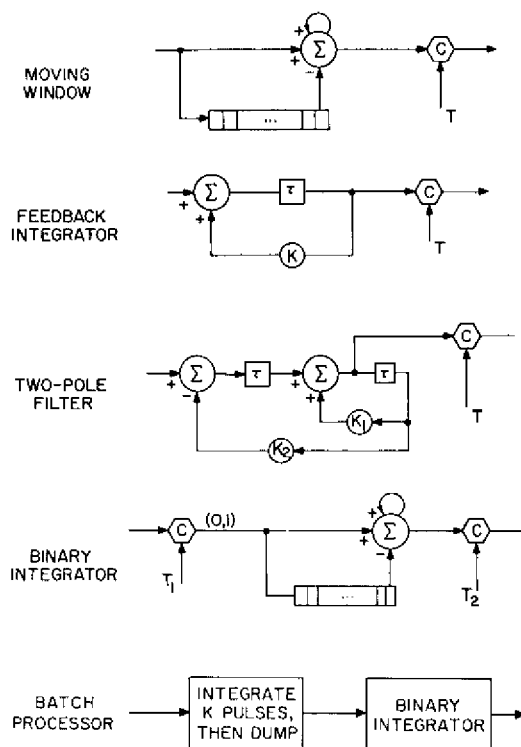


Fig. 16 — Common integrators

tained by either taking the maximum value of the running sum or taking the midpoint between the first and last crossing of the detection threshold. Both methods have a bias of  $N/2$  pulses which is easily corrected. The standard deviation of the estimation error of both estimators is about 20% higher than the Cramer-Rao lower bound. The major disadvantage of this detector is that the last  $N$  pulses for each range cell must be saved. For radars with large beamwidths and thus many pulses, the moving window requires extensive hardware. However with the lower cost and size of memory this disadvantage is rapidly disappearing.

*Feedback integrator*

The amount of storage required can be reduced significantly by using a feedback integrator, which requires the storage of only one number. Although the feedback integrator applies an exponential weighting into the past, its detection performance is only 1 dB less than the optimal integrator. Unfortunately difficulties are encountered when using the feedback integrator to estimate the azimuth position. The threshold-crossing procedure yields estimates only 20% greater than the lower bound, but the bias is a function of  $S/N$  and must be estimated. On the other hand the maximum value, although having a constant bias, has estimates which are 100% greater than the lower bound. This author's opinion is that this detector has limited utility.

*Two-pole filter*

The two-pole filter requires the storage of an intermediate calculation in addition to the integrated output. However with this rather simple device a weighting pattern similar to the antenna pattern can be obtained; consequently good performance would be expected. The detection performance is within 0.15 dB of the optimal detector, and its angular estimates are about 20% greater than the Cramer-Rao lower bound. If the desired number of pulses integrated is changed (because of change in rotation of the radar or use of another radar), it is necessary to change only the feedback values  $K_1$  and  $K_2$ . Their optimal values are set by

$$K_1 = 2 e^{-\psi \omega_d \tau / \sqrt{1 - \psi^2}} \cos(\omega_d \tau) \quad (48)$$

and

$$K_2 = e^{-2\psi \omega_d \tau / \sqrt{1 - \psi^2}}, \quad (49)$$

where  $\psi = 0.63$ ,  $N\omega_d \tau = 2.2$ , and  $N$  is the number of pulses between the 3-dB points of the antenna.

*Binary Integrator*

The binary integrator is also known as the dual-threshold detector,  $M$ -out-of- $N$  detector, or rank detector. The input samples are quantized to 0 or 1 depending on whether or not they are less than a threshold  $T_1$ . The last  $N$  zeros and ones are summed and compared to a second (detection) threshold  $T_2 = M$ . The detection performance of this detector is 2 dB less than the moving-window integrator because of the hard limiting of the data, and the angular estimation error is 25% greater than the Cramer-Rao lower bound. This detector is used because it is easily implemented, it ignores interference spikes which cause trouble with integrators that directly use signal amplitude, and it works extremely well when\*† the noise has a non-Rayleigh density.

A comparison of the binary integrator (three out of three), the median detector (two out of three), and the mean detector (moving window) in log-normal interference is shown in Fig. 17. The optimal binary integrator is much better than straightforward integration. The optimal values for the second threshold were found by Schwartz‡ for Rayleigh interference and by Schleher§ for log-normal interference.

*Batch Processor*

The batch processor is used when there are a large number of pulses in the 3-dB beamwidth. If  $KN$  pulses are in the 3-dB beamwidth,  $K$  pulses are summed and either a 0 or 1 is declared depending on whether or not the sum is less than a threshold  $T_1$ . The last  $N$  zeros and ones are summed and compared to a second threshold  $M$ .

\*D. C. Schleher, IEEE 1975 International Radar Conf., 262-267, 1975.

†G. V. Trunk, "Non-Rayleigh Sea Clutter: Properties and Detection of Targets," NRL Report 7986, June 1976.

‡M. Schwartz, IEEE Trans. Information Theory 2, 135-139 (1956).

§D. C. Schleher, IEEE 1975 International Radar Conf., 262-267, 1975.

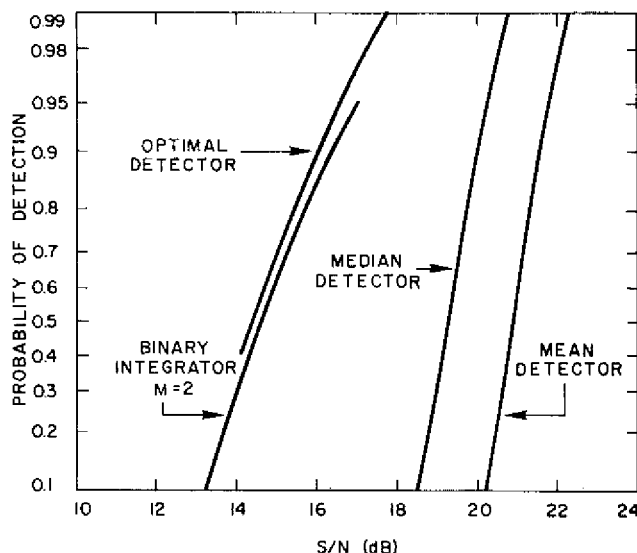


Fig. 17 — Comparison of various detectors in log-normal interference ( $N = 3$ ,  $P_{fa} = 10^{-6}$ )

The batch processor, like the binary integrator, is easily implemented, ignores interference spikes, and works extremely well when the noise has a non-Rayleigh density, but furthermore in comparison with the binary integrator the batch processor requires less storage, detects better (less than 2 dB from moving window), and estimates angles more accurately.

The batch processor has been implemented by the Applied Physics Laboratory\* of Johns Hopkins University with great success. To obtain a more accurate azimuth estimate, they use

$$\hat{\theta} = \frac{\sum A_i \theta_i}{\sum A_i}, \quad (50)$$

where  $A_i$  are the amplitudes of the sums greater than  $T_1$  and  $\theta_i$  are the corresponding antenna azimuth angles. When many pulses are on target ( $N > 20$ ), this detector is generally favored by this author.

### False Alarms

If fixed thresholds are used with the previously discussed integrators, the detectors will saturate the tracking computer associated with the system and disrupt the system. Three important facts should be remembered:

- It makes little sense to have an automatic detection system without an associated tracking system;
- The sensitivity of the detector should be as high as possible without saturating the tracking computer;

\*"Radar Processing Subsystem Evaluation", Vol. I, APL Report FP8-T-013, Nov. 1975.

- False alarms and false targets are not a problem if they are removed by the tracking computer. Tracking (scan-to-scan processing) is the only way to remove stationary point clutter or target MTI residues.

One can reduce the number of false alarms with a fixed-threshold system by setting a high threshold, but this would reduce sensitivity in regions of low-noise (clutter) return. A detector is required which will detect a target when it has a higher return than its immediate background. Two such types of detectors are adaptive-thresholding and nonparametric detectors. Both of these detectors assume that the samples in the range cells surrounding the test cell (called reference or neighboring cells) are independent and identically distributed; furthermore it is usually assumed that the time samples are independent. Both detectors test whether the test cell has a return sufficiently larger than the reference cells. A survey of CFAR procedures can be found in Hansen\*.

#### *Adaptive Thresholding*

The basic assumption of the adaptive-thresholding technique is that the noise density is known except for a few unknown parameters. The surrounding reference cells are used to estimate the unknown parameters, and a threshold based on the estimated density is then obtained. The simplest adaptive detector is the cell-averaging CFAR investigated by Finn and Johnson†. If the noise has a Rayleigh density, only the parameter  $\sigma$  needs to be estimated, since the mean of a Rayleigh distribution is  $\sigma\sqrt{\pi/2}$  and the variance is  $\sigma^2(2v-\pi/2)$ . Thus, by estimating the mean, one obtains an estimate  $\hat{\sigma}$  which can be used to set a threshold  $T$  to yield the desired  $P_{fa}$ . However, since  $T$  is set by an estimate  $\hat{\sigma}$ , it must be slightly larger than the threshold one would use if  $\sigma$  were known a priori. The raised threshold causes a loss in target sensitivity and is referred to as a CFAR loss. This loss has been calculated by Mitchell and Walker‡, and some results are summarized in Table 2. As can be seen, for a small number of reference cells, the loss is large because of the poor estimate of  $\sigma$ .

This thresholding technique is more effective in maintaining CFAR when it is applied to the binary integrator or batch processor, as shown in Fig. 18. This is because when the number of pulses integrated by the binary integrator is moderate, the  $P_{fd}$  on a single pulse is rather large; for example  $P_{fa} = 0.1$  for a single pulse yields  $P_{fa} = 10^{-5}$  for a seven-out-of-ten integrator. Thus, since most non-Rayleigh densities are Rayleigh-like to the 10th percentile, this type of processor will maintain a low  $P_{fa}$  in most non-Rayleigh environments. This demonstrates a general rule: to maintain a low  $P_{fa}$  in various environments, adaptive thresholding should be placed in front of the integrator. For any noise distribution, CFAR can be maintained by counting the number of ones out of the comparator per scan and using this number to control  $K$ ; that is, if the number is too large,  $K$  is increased.

Front-end thresholding, which maintains amplitude information by dividing the average reference value into the test cell, was investigated by Hansen and Ward§ and is shown in Fig. 19. This type of processing is especially effective when there is strong interference which is variable on a pulse-to-pulse basis.

\*V. G. Hansen, IEEE International Conference on Radar — Present and Future, 325-332, 1973.

†H. M. Finn and R. S. Johnson, RCA Review 29, 414-464 (1968).

‡R. L. Mitchell and J. K. Walker, IEEE Trans. Aerospace and Electronic Systems AES-7, 671-676 (1971).

§V. G. Hansen and H. R. Ward, IEEE Trans. Aerospace and Electronic Systems 8, 648-652 (1972).

Table 2 — CFAR Loss for  $P_{fa} = 10^{-6}$  and  $P_D = 0.9$

Number of Pulses Integrated	Loss for Various Numbers of Reference Cells (dB)					
	1	2	3	5	10	$\infty$
1	-	-	15.3	7.7	3.5	0
3	-	7.8	5.1	3.1	1.4	0
10	6.3	3.3	2.2	1.3	0.7	0
30	3.6	2.0	1.4	1.0	0.5	0
100	2.4	1.4	1.0	0.6	0.3	0

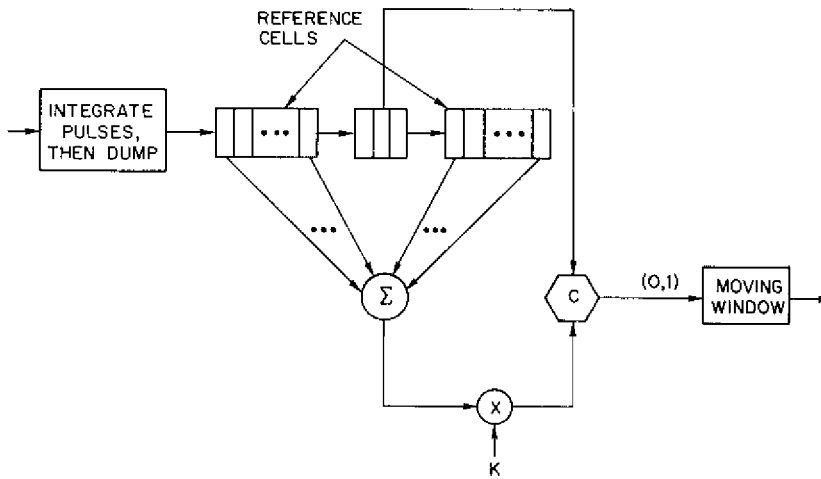


Fig. 18 — Cell-averaging CFAR implemented with the batch processor

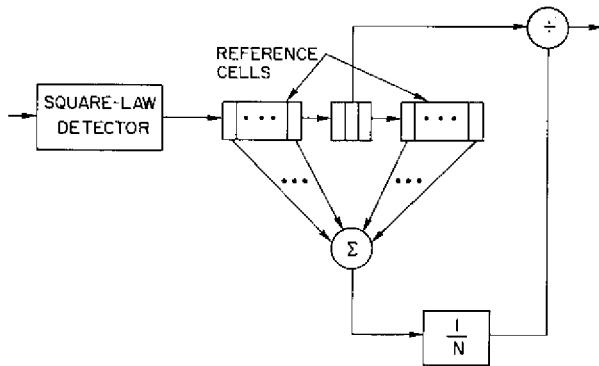


Fig. 19 — Front-end cell-averaging CFAR receiver

When the noise has a non-Rayleigh density, such as the chi-square density or log-normal density, two parameters must be estimated, and the adaptive detector is more complicated. If several pulses are integrated with any of the amplitude integrators, the integrated output will be approximately Gaussian distributed. Then the two parameters which must be estimated are the mean and the variance. These estimates are given by

$$\bar{X} = \frac{1}{N} \sum_t x_t, \quad (51)$$

and

$$\hat{\sigma}^2 = \frac{1}{N} \sum_t x_t^2 - \bar{X}^2 \quad (52)$$

where the summation is over the  $N$  range cells surrounding the test cell.

When successive pulses in the same range cell are correlated (as with returns from rain or sea clutter), many false alarms will occur if only the mean value (51) is estimated. A threshold of the form

$$T = \bar{X} + K\hat{\sigma} \quad (53)$$

will provide a low  $P_{fa}$  for the amplitude integrators: moving window, feedback integrator, and two-pole filter. Nothing can be done to the binary integrator to yield a low  $P_{fa}$  in correlated noise; thus it should not be used in this situation. On the other hand, if the correlation time is less than a batching interval, the batch processor will yield a low  $P_{fa}$  without modifications.

#### *Nonparametric Detectors*

The most common way nonparametric detectors obtain CFAR is by ranking the test sample with the reference cells. Under the hypothesis that all the samples are independent samples from an unknown density function, the test sample has a uniform density function. For instance, with reference to the rank detector in Fig. 20, the test cell is compared to 15 of its neighbors. Since in the set of 16 samples the test sample has equal probability of being the smallest sample (rank = 0 or equivalently any other rank), the probability that the test sample takes on values 0, 1, ..., 15 is 1/16. A simple rank detector\* can be constructed by comparing the rank (number of reference cells that the test cell exceeds) to a threshold  $K$ ; and the output is 1 if the rank is larger and 0 otherwise. The zeros and ones are summed in a moving window. This detector incurs a CFAR loss of about 2 dB and is extremely effective, if the time samples are independent. Only certain values of  $P_{fa}$  can be obtained. Thus, if the number of pulses integrated is small, low  $P_{fa}$  values cannot be obtained.

If the time samples are dependent, the rank detector will not yield CFAR. A modified rank detector, called the modified generalized sign test† (MGST) is an attempt to maintain a low  $P_{fa}$  and is that shown in Fig. 20. This detector can be divided into three parts: a ranker, an integrator (in this case a two-pole filter), and a thresholding device. A target is declared when the integrated output exceeds two thresholds. The first threshold is fixed (equals  $\mu + T_1/K$  from Fig. 20) and yields CFAR when the reference cells are independent and identically distributed. The second threshold is adaptive and maintains a low  $P_{fa}$  when the

\*V. G. Hansen and B. A. Olsen, IEEE Trans. Aerospace and Electronic Systems 4, 942-950 (1971).

†G. V. Trunk, B. H. Cantrell, and F. D. Queen, IEEE Trans. Aerospace and Electronic Systems 10, 574-582 (1974).

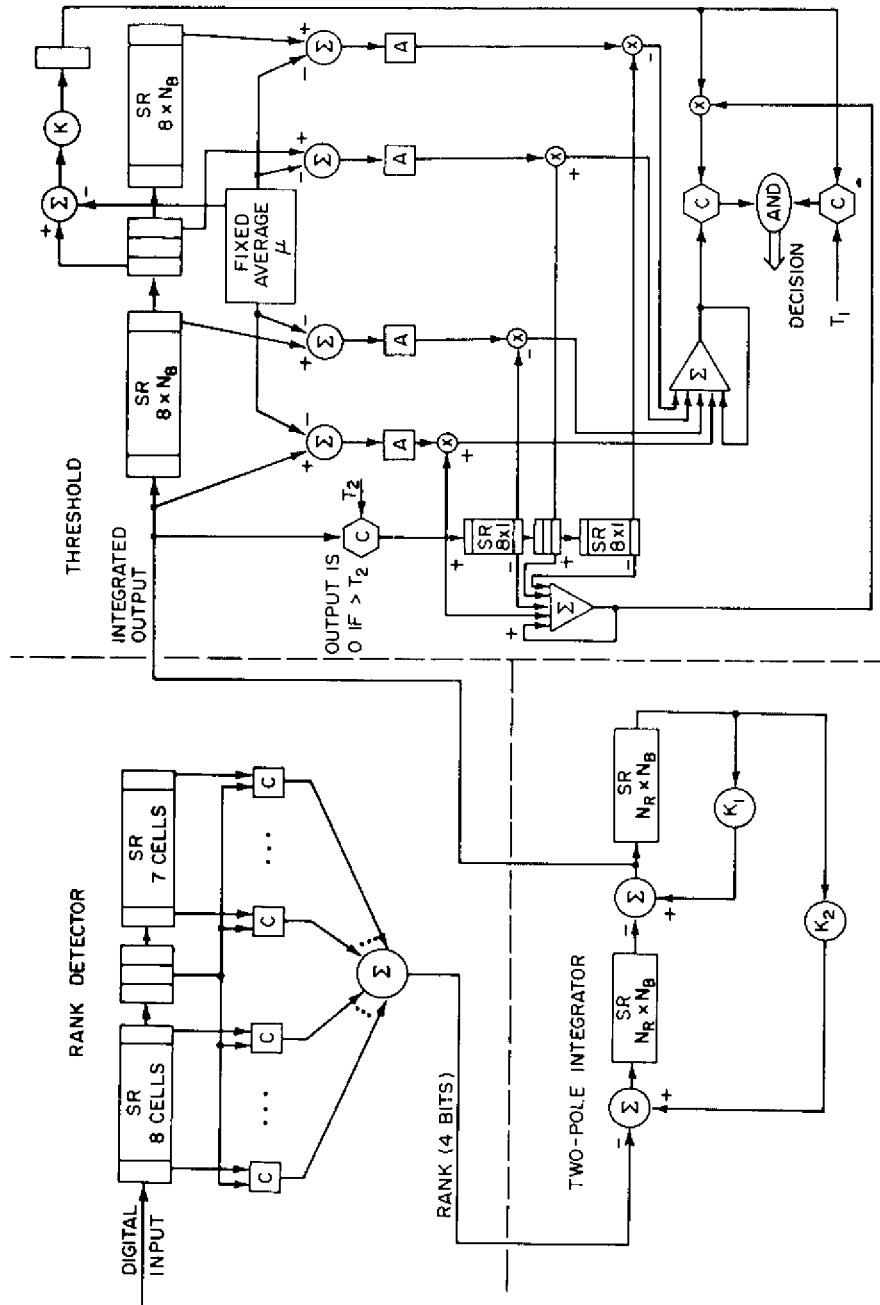


Fig. 20 — Modified generalized sign-test processor. (SR indicates shift register, and A indicates absolute value.) (From G. V. Trunk, B. H. Cantrell, and F. D. Queen, IEEE Trans. Aerospace and Electronic Systems AES-10, 574-582, 1974, courtesy of the Institute of Electrical and Electronics Engineers.)

reference samples are correlated. The device uses the mean-deviate estimate, where extraneous targets in the reference cells have been excluded from the estimate by use of a preliminary threshold  $T_2$ , to estimate the standard deviation of the correlated samples.

The rank and MGST detectors are basically two-sample detectors. They decide a target is present if the ranks of the test cell are significantly greater than the ranks of the reference cells. Target suppression occurs at all interfaces (such as a land-and-sea interface), where the homogeneity assumption is violated. However, some tests exist (Hansen\* investigated the Spearman Rho and Kendall Tau tests) which depend on only the test cell. These tests work on the fact that, as the antenna beam sweeps over a point target, the signal return increases and then decreases. Thus for the test cell the ranks should follow a pattern first increasing and then decreasing. Although these detectors do not require reference cells and hence have the useful property of not requiring homogeneity, these detectors are not generally used because of the large CFAR loss taken for moderate sample sizes: for  $N = 16$  the loss is 10 dB, and for  $N = 32$  the loss is 6 dB.

The paper by Hansen\* is worth noting because it introduced the concept of importance-sampling for calculation of false-alarm thresholds. The fundamental principle of the importance-sampling technique is to modify the probabilities that govern the outcome of the basic experiment of the simulation in such a way that the event of interest (the false alarm) occurs more frequently. This distortion is then compensated for by weighting each event by the ratio of the probability that this specific event would have occurred if the true probabilities had been used in the simulation to the probability that this event would occur with the distorted probabilities. Consequently by proper choice of the distorted probabilities the number of repetitions can be reduced greatly. Further details on importance sampling can be found in Trunk et al.†, Hansen‡, and Hillier and Lieberman§.

In summary, when only a small number of returns are available (less than eight), amplitude information must be used, and this author favors the moving-window integrator. When a moderate number (between eight and 20) are available, a rank detector should be used if samples are independent; and a two-pole filter with thresholding of the form  $T = \bar{X} + K\sigma$  should be used if the samples are dependent. If a large number of pulses (greater than 20) are available, the batch processor or MGST processor should be used. These rules should serve only as a general guideline. It is highly recommended that a sample of the radar environment be collected and analyzed and that various detectors be simulated on a computer and tested against recorded data.

### Sequential Detectors

Sequential detectors, which can be used with phased-array radars, are based on the idea that in many cases, depending on the returned samples, a decision can be made on a few sam-

\*V. G. Hansen, *IEEE Trans. Information Theory* **IT-16**, 309-318 (1970).

†G. V. Trunk, B. H. Cantrell, and F. D. Queen, *IEEE Trans. Aerospace and Electronic Systems* **10**, 574-582 (1974).

‡V. G. Hansen, *Computer and Electrical Eng.* **1**, 545-550 (1974).

§F. S. Hillier and G. J. Lieberman, *Introduction to Operations Research*, Holden-Day, New York, 457-459 (1967).

ples. The sequential likelihood-ratio test (SLRT) works as follows: given independent samples  $x_1, \dots, x_m$ , calculate the likelihood ratio

$$L_m = \frac{p(x_1, \dots, x_m | H_1)}{p(x_1, \dots, x_m | H_0)} \quad (54)$$

If  $L_m \geq A$ , accept  $H_1$  (target present); if  $L_m \leq B$ , accept  $H_0$  (no target present); and if  $B < L_m < A$ , take another sample. The SLRT has the useful properties that the thresholds are set by the simple formulas  $A = P_D/P_{fa}$  and  $B = (1 - P_D)/(1 - P_{fa})$  and that for all tests with a given  $P_D$  and  $P_{fa}$  the SLRT requires the smallest average sample size. Further details about the SLRT can be found in Lindgren\*.

An early application of sequential detection to radar was discussed by Marcus and Swerling†. Unfortunately, in radar the application of SLRT is not straightforward, since one is required to make a decision in every range cell before the test can be ended and the agile beam moved. The modified problem considered was

$H_0$ : noise present in all range cells

or

$H_1$ : exactly one signal present in the  $i$ th range cell ( $i$  unknown).

They performed some numerical calculations and concluded that:

- The greatest savings in average sample size comes when no signal is present ( $H_0$  true);
- In comparison with a fixed-sample-size test, SLRT provides a greater savings when the number of range cells is small and when S/N is small;
- It is not necessary to truncate the test.

## TRACKING SYSTEM

Track-while-scan systems (tracking systems for surveillance radars whose nominal scan time is from 4 to 12 s) will now be considered. If the probability of detection ( $P_D$ ) per scan is high, if accurate measurements are made, if the target density is low, and if there are few false detections (crossings of a threshold, with no judgment being made on whether or not it belongs to a valid target), the design of the correlation logic and tracking filter is straightforward. However in a realistic radar environment these assumptions are never valid, and the design problem is complicated.

White and Silberman‡ list many problems encountered in actual situations. Among these problems are target fades (due to multipath propagation, clutter masking, interference, blind

\*B. W. Lindgren, *Statistical Theory*, MacMillan, New York, 1962.

†M. B. Marcus and P. Swerling, *IEEE Trans. Information Theory* 8, 237-245 (1962).

‡D. M. White and S. R. Silberman, "Simulation of 2D Radar Automatic Detection and Tracking Systems: Baseline Program," Technology Service Corporation, TSC-W8-60, Aug. 1975.

speeds, and atmospheric conditions), false alarms (due to noise, clutter, interference, and jamming), and poor radar parameter estimates (due to noise, unstabilized radar platforms, unresolved targets, target splits (two detections for a single target), multipath propagation, and propagation effects).

A general outline of a track-while-scan system will be considered first. Then the tracking filter, maneuver-following logic, track initiation, and correlation logic will be discussed in detail. Finally, methods of integrating data from several radars will be discussed.

### System Outline

Almost all track-while-scan systems operate on a sector basis. A typical series of operations is shown in Fig. 21. For instance, if the radar has reported all the detections in sector 11 and is now in sector 12, the tracking program would start by correlating (trying to associate) the clutter points (stationary tracks) in sector 10 with detections in sectors 9, 10, and 11. Those detections that are associated with clutter points are deleted (are not used for further correlations) from the detection file and are used to update the clutter points. Updating clutter points usually implies replacing the old point by the associated detection.

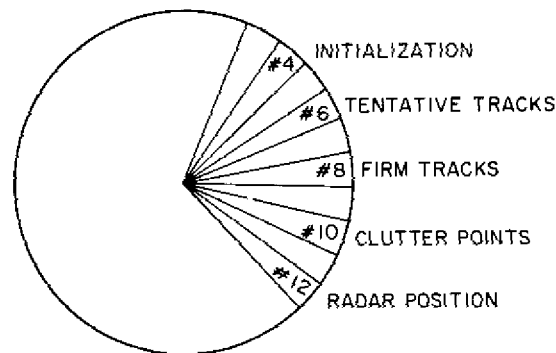


Fig. 21 — Various operations of a track-while-scan system performed on a sector basis

Next, firm tracks in sector 8 are correlated with detections in sectors 7, 8, and 9. By this time all clutter points have been removed from sectors 9 and below. Those detections which are associated with firm tracks are deleted from the detection file and are used to update the appropriate track. The filter for performing this updating will be described in the next subsection.

Usually, some provision is made for giving preference to firm tracks (with respect to tentative tracks) in the correlation process. By performing the correlation process two sectors behind firm track correlations (Fig. 21), it is impossible for tentative tracks to steal detections belonging to firm tracks. In other tracking systems the correlation for firm and tentative tracks is performed in the same sector; however the generalized distance  $D$  between tracks and detections is incremented by  $\Delta D$  if the track is tentative.

Finally detections which are not associated with either clutter points or tracks are used for initiation purposes. The most common initiation procedure is to initiate a tentative track;

later the track is dropped or else made a firm track or clutter point. Cantrell et al.\* suggest that both a clutter point and tentative track be established. If the detection came from a stationary target, the clutter point will be updated and the tentative track will eventually be dropped. On the other hand, if the detection came from a moving target, the tentative tracks will be made firm and the clutter point will be dropped. The latter method requires less computer computation time when most of the detections are clutter residues.

The correlation procedure is made in a sector framework to avoid the necessity of correlating all tracks with all detections. The procedure can be implemented very easily by defining two computer arrays: a sector file and a track file. The sector file for sector I contains the first track number in sector I, and the track file for track J contains the next track number in the same sector as track J or a zero, indicating that the track is the last track in the sector. Further information about the details of a tracking system can be found in Cantrell et al.†, Wilson and Cantrell‡, and Trunk et al.§.

### Tracking Filters

Before proceeding, the coordinate system in which the tracking will be performed will be discussed. The quantities measured by the radar are spherical: range, azimuth, elevation, and possibly range rate. Thus it may seem natural to perform tracking in spherical coordinates. However this causes difficulties, since motion of constant-velocity targets (straight lines) will cause acceleration terms in all coordinates. A simple solution to this problem is to track in a Cartesian coordinate system. While it may appear that the appropriate transformations ( $x = R \cos \theta_e \cos \theta_a$ , etc. where  $R$  is the range,  $\theta_e$  is the elevation angle, and  $\theta_a$  is the azimuth angle) will destroy the accurate range track, Cantrell# has shown that the inherent accuracy is maintained. Quigley and Holmes\*\* note that maneuvering targets cause a large range error but a rather insignificant azimuth error and thus suggest using a target-oriented Cartesian coordinate system. Specifically, the  $x$  axis is taken along the azimuth direction of the target and the  $y$  axis is taken in the cross range direction.

Skalansky†† performed one of the first analyses of the tracking filter for a track-while-scan system. He considered the  $\alpha - \beta$  filter described by

$$x_s(k) = x_p(k) + \alpha [x_m(k) - x_p(k)], \quad (55)$$

$$V_s(k) = V_s(k-1) + \beta [x_m(k) - x_p(k)]/T, \quad (56)$$

\*B. H. Cantrell, G. V. Trunk, F. D. Queen, J. D. Wilson, and J. J. Alter, IEEE 1975 International Radar Conference, 391-395, 1975.

†B. H. Cantrell, G. V. Trunk, and J. D. Wilson, "Tracking System for Two Asynchronously Scanning Radars," NRL Report 7841, Dec. 1974.

‡J. D. Wilson and B. H. Cantrell, "Tracking System for Asynchronously Scanning Radars with New Correlation Techniques and an Adaptive Filter," NRL Report 7952, Jan. 1976.

§G. V. Trunk, J. D. Wilson, B. H. Cantrell, J. J. Alter, and F. D. Queen, "Modifications to and Preliminary Results for the ADIT System", NRL Report 8091, Apr. 1977.

#B. H. Cantrell, "Description of an  $\alpha - \beta$  Filter in Cartesian Coordinates," NRL Report 7548, Mar. 1973.

\*\*A. L. Quigley and J. E. Holmes, "The development of Algorithms for the Formation and Updating of Tracks," Admiralty Surface Weapons Establishment, WP-XBC-7512, Portsmouth P06 4AA, Nov. 1975.

††J. Skalansky, RCA Review 18, 163-185 (1957).

and

$$x_p(k+1) = x_s(k) + V_s(k)T, \quad (57)$$

where  $x_s(k)$  is the smoothed position,  $V_s(k)$  is the smoothed velocity,  $x_p(k)$  is the predicted position,  $x_m(k)$  is the measured position,  $T$  is the scanning period (time between detections), and  $\alpha$  and  $\beta$  are the system gains.

The optimal filter for performing the tracking when the equation of motion is known is the Kalman filter, first discussed by Kalman\* and later by Kalman and Bucy†. The Kalman filter is a recursive filter which minimizes the least-square error. The state equation in  $xy$  coordinates for a constant-velocity target is‡

$$X(t+1) = \phi(t) X(t) + \Gamma(t) A(t), \quad (58)$$

where

$$X(t) = \begin{bmatrix} x(t) \\ \dot{x}(t) \\ y(t) \\ \dot{y}(t) \end{bmatrix}, \quad \phi(t) = \begin{bmatrix} 1 & T & 0 & 0 \\ 0 & 1 & 0 & 0 \\ 0 & 0 & 1 & T \\ 0 & 0 & 0 & 1 \end{bmatrix},$$

$$\Gamma(t) = \begin{bmatrix} T^2/2 & 0 \\ T & 0 \\ 0 & T^2/2 \\ 0 & T \end{bmatrix}, \quad \text{and } A(t) = \begin{bmatrix} a_x(t) \\ a_y(t) \end{bmatrix},$$

with  $X(t)$  being the state vector at time  $t$  consisting of position and velocity components  $x(t)$ ,  $\dot{x}(t)$ ,  $y(t)$ , and  $\dot{y}(t)$ ;  $t+1$  being the next observation time;  $T$  being the time between observations; and  $a_x(t)$  and  $a_y(t)$  being random accelerations with covariance matrix  $Q(t)$ . The observation equation is

$$Y(t) = M(t) X(t) + V(t), \quad (59)$$

where

$$Y(t) = \begin{bmatrix} x_m(t) \\ y_m(t) \end{bmatrix}, \quad M(t) = \begin{bmatrix} 1 & 0 & 0 & 0 \\ 0 & 0 & 1 & 0 \end{bmatrix}, \quad \text{and } V(t) = \begin{bmatrix} v_x(t) \\ v_y(t) \end{bmatrix},$$

with  $Y(t)$  being the measurement at time  $t$  consisting of positions  $x_m(t)$  and  $y_m(t)$  and  $V(t)$  being a zero-mean noise whose covariance matrix is  $R(t)$ .

The problem is solved recursively by first assuming the problem is solved at time  $t-1$ . Specifically, it is assumed that the best estimate  $\hat{X}(t-1|t-1)$  at time  $t-1$  and its error covariance matrix  $P(t-1|t-1)$  are known, where the caret in the expression of the form  $\hat{X}(t|s)$  signifies an estimate and the overall expression signifies  $X(t)$  is being estimated with observations up to  $Y(s)$ . The six steps involved in the recursive algorithm are

1. Calculate the one-step prediction

$$\hat{X}(t|t-1) = \phi(t-1)\hat{X}(t-1|t-1); \quad (60)$$

\*R. E. Kalman, Trans. ASME Series D, J. Basic Engineering 82, 35-45 (1960).

†R. E. Kalman and R. S. Bucy, Trans. ASME Series D, J. Basic Engineering 83, 95-107 (1961).

‡F. R. Castella and E. G. Dunnebacke, IEEE Trans. Aerospace and Electronic Systems 10, 891-895 (1974).

2. Calculate the covariance matrix for the one-step prediction

$$P(t|t-1) = \phi(t-1)P(t-1|\phi^T(t-1) + \Gamma(t-1)Q(t-1)\Gamma^T(t-1); \quad (61)$$

3. Calculate the predicted observation

$$\hat{Y}(t|t-1) = M(t)\hat{X}(t|t-1); \quad (62)$$

4. Calculate the filter gain

$$\Delta(t) = P(t|t-1)M^T(t)[M(t)P(t|t-1)M^T(t) + R(t)]^{-1}; \quad (63)$$

5. Calculate the new smoothed estimate

$$\hat{X}(t|t) = \hat{X}(t|t-1) + \Delta(t)[Y(t) - \hat{Y}(t|t-1)]; \quad (64)$$

6. Calculate the new covariance matrix

$$P(t|t) = [I - \Delta(t)M(t)]P(t|t-1). \quad (65)$$

In Summary, with an estimate  $\hat{X}(t-1|t-1)$  and its covariance matrix  $P(t-1|t-1)$  as the start, after a new observation  $Y(t)$  is received and the six quantities in the recursive algorithm are calculated, a new estimate  $\hat{X}(t|t)$  and its covariance matrix  $P(t|t)$  are obtained.

It is fairly simple to show that for a zero random acceleration,  $Q(t) \equiv 0$  and a constant measurement covariance matrix  $R(t) = R$ , the  $\alpha$ - $\beta$  filter can be made equivalent to the Kalman filter by setting

$$\alpha = \frac{2(2k-1)}{k(k+1)} \quad (66)$$

and

$$\beta = \frac{6}{k(k+1)} \quad (67)$$

on the  $k$ th scan.\*

Thus as time passes,  $\alpha$  and  $\beta$  approach zero, applying heavy smoothing to the new samples. This method is optimal for straight-line tracks but must be modified to enable the filter to follow target maneuvers.

### Maneuver-Following Logic

Benedict and Bordner† noted that in track-while-scan systems there is a conflicting requirement between good noise smoothing (implying small  $\alpha$  and  $\beta$ ) and good maneuver-following capability (implying large  $\alpha$  and  $\beta$ ). Although some compromise is always required, the smoothing equations should be constructed to give the "best" compromise for a desired

\*A. L. Quigley, IEEE International Conference on Radar — Present and Future, 352-357, 1973.

†T. R. Benedict and G. W. Bordner, IEEE Trans. Automatic Control AC-7 (No. 4), 27-32 (1962).

noise reduction. Specifically, since the variance-reduction ratio  $K$ , defined as the steady-state variance in the filter position output divided by the variance in the measured position, equals

$$K = \frac{2\alpha^2 + \beta(2 - 3\alpha)}{\alpha[4 - \beta - 2\alpha]}, \quad (68)$$

the  $(\alpha, \beta)$  pair should be chosen to satisfy (68) and maximize the maneuver-following capability. Benedict and Bordner\* defined a measure of transient-following capability and showed that  $\alpha$  and  $\beta$  should be related by

$$\beta = \frac{\alpha^2}{2 - \alpha}. \quad (69)$$

Alternately an  $(\alpha, \beta)$  pair satisfying (69) can be chosen so that the tracking filter will follow a specified  $g$  turn. Cantrell† developed a method of determining the probability that the target detection will fall within a correlation region centered at the predicted target position when the target is performing a specified  $g$ -turn. Then the  $(\alpha, \beta)$  pair yielding the smallest correlation region should be used.

The trouble with the preceding method is that if high- $g$  turns are followed the noise performance is rather poor. To rectify this situation, a turn detector employing the two correlation regions shown in Fig. 22 is used. If the detection is in the nonmaneuvering correlation region, the filter operates as usual,  $\alpha$  and  $\beta$  being reduced according to (66) and (67). Usually it is worthwhile to bound  $\alpha$  and  $\beta$  from zero by assuming a random acceleration  $Q(t) \neq 0$  corresponding to approximately a 1- $g$  maneuver. When the target falls outside the inner gate but within the maneuver gate, a maneuver is declared and the filter bandwidth is increased ( $\alpha$  and  $\beta$  are increased); Quigley and Holmes‡ increase the bandwidth by lowering the value of  $k$  in (66) and (67). To avoid the problem of the target fading and a false alarm appearing in the large maneuver gate, the track should be bifurcated when a maneuver is declared. That is, two tracks are generated: the old track with no detection and a new *maneuvering* track with the new detection and increased bandwidth. The next detection is used to resolve the ambiguity and remove one of the tracks.

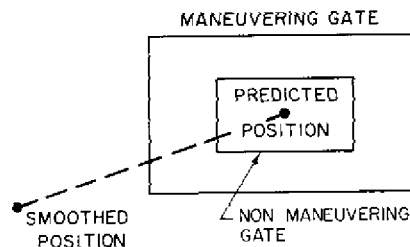


Fig. 22 — Maneuver and nonmaneuver gates centered at the target's predicted position

\*T. R. Benedict and G. W. Bordner, IEEE Trans. Automatic Control AC-7 (No. 4), 27-32 (1962).

†B. H. Cantrell, "Behavior of  $\alpha - \beta$  Tracker for Maneuvering targets Under Noise, False Target, and Fade Conditions," NRL Report 7434, Aug. 1972.

‡A. L. Quigley and J. E. Holmes, "The development of Algorithms for the Formation and Updating of Tracks," Admiralty Surface Weapons Establishment, WP-XBC-7512, Portsmouth P06 4AA, Nov. 1975.

Cantrell et al.\* suggested that the  $\alpha - \beta$  filter (described by (55), (56), and (57)) be made adaptive by adjusting  $\alpha$  and  $\beta$  by

$$\alpha = 1 - e^{-2\xi\omega_0 T} \quad (70)$$

and

$$\beta = 1 + e^{-2\xi\omega_0 T} - 2e^{-\xi\omega_0 T} \cos(\omega_0 T \sqrt{1 - \xi^2}), \quad (71)$$

in which

$$\omega_0 = 0.5|p_1(k)/p_2(k)|, \quad (72)$$

where

$$p_1(k) = e^{-\omega_a T} p_1(k-1) + (1 - e^{-\omega_b T}) \epsilon(k)\epsilon(k-1) \quad (73)$$

and

$$p_2(k) = e^{-\omega_b T} p_2(k-1) + (1 - e^{-\omega_b T}) \epsilon(k)\epsilon(k) \quad (74)$$

with  $\xi$  being the damping coefficient (nominally 0.7),  $T$  being the time since the last update,  $\omega_a$  and  $\omega_b$  being weighting constants, and  $\epsilon(k)$  being the error between the measured and predicted positions on the  $k$ th update. The basic principle of the filter is that  $p_1(k)$  is an estimate of the covariance of successive errors and  $p_2(k)$  is an estimate of the error variance. When the target trajectory is a straight line,  $p_1(k)$  approaches 0, since the expected value of  $\epsilon(k)$  is 0. Thus  $\omega_0$  approaches 0, and the filter performs heavy smoothing. When the target turns,  $p_1(k)$  grows, since the error  $\epsilon(k)$  will have a bias (either positive or negative). Thus  $\omega_0$  grows, and the filter can follow the target maneuver.

Another solution to the target-maneuvering problem is due to Singer†, who suggested using the Kalman filter with a realistic target-maneuvering model. He assumed that the target was moving at a constant velocity but was being perturbed by a random acceleration. Since the target acceleration is correlated in time (if the target is accelerating at time  $t$ , it is likely to be accelerating at time  $t + \Delta t$ ), it was assumed that the covariance of the correlation was

$$r(\tau) = E\{a(t)a(t+\tau)\} = \sigma_m^2 e^{-\alpha|\tau|}, \quad (75)$$

where  $a(t)$  is the target acceleration at time  $t$ ,  $\sigma_m^2$  is the variance of the target acceleration, and  $\alpha$  is the reciprocal of the maneuver time constant. The density function for target acceleration consists of delta functions at  $\pm A_{\max}$ , each with probability  $P_{\max}$ , a delta function at 0 with probability  $P_0$ , and a uniform density between  $-A_{\max}$  and  $A_{\max}$ . For this density

$$\sigma_m^2 = \frac{A_{\max}^2}{3} (1 + 4P_{\max} - P_0). \quad (76)$$

For this target motion Singer† then calculated the state transition matrix  $\phi(t)$  and the covariance matrix  $Q(t)$ , thereby specifying the Kalman-filter solution. He generated curves which

\*B. H. Cantrell, G. V. Trunk, F. D. Queen, J. D. Wilson, and J. J. Alter, IEEE 1975 International Radar Conference, 391-395, 1975.

†R. A. Singer, IEEE Trans. Aerospace and Electronic Systems AES-6, 473-483 (1970).

give the steady-state performance of the filter for any data rate, single-look measurement accuracies, encounter geometry, and class of maneuvering targets.

### Track Initiation

Detections that do not correlate with clutter points or update tracks are used to initiate new tracks. If the detection does not contain doppler information, the new detection is used as the predicted position, and a large correlation region must be used. The probability of false alarms being in the large correlation region is large; hence tracks should not be declared firm until a third detection (falling within a smaller correlation region) is obtained. The usual initiation criteria are three out of four and three out of five. The possible exceptions are when doppler information is available (so that a small correlation region can be used immediately) or for pop-up (close) targets in a military situation.

Quigley and Holmes\* suggest using a sequential hypothesis-testing scheme for initiating tracks. When a correlation is made on the  $i$ th scan,  $\Delta_i$  is added to the likelihood; and when a correlation opportunity is missed,  $\Delta_i$  is subtracted from the likelihood. The increment  $\Delta_i$  is set by the state of the tracking system, being a function of the closeness of the association, the number of false alarms, the a-priori probability of targets, and the probability of detection. Although this method will inhibit false tracks in dense detection environments, it will not necessarily establish the correct tracks. The proper solution will probably be a method of generating trial tracks using detections from the last several scans and then eliminating the false tracks in an easily implementable manner.

To initiate tracks with detections from unsynchronized radars, Trunk et al.† suggest that two times, namely  $T_D$  and  $T_F$ , be used. If time  $T_D$  goes by between track updates, the tentative track should be dropped; and if the track is updated after a time  $T_F$  after initialization, the tentative track should be made firm. Setting  $T_F > T_D$  insures that three detections are required for making a track firm.

Firm tracks that are not updated in 30 or 40 seconds are usually dropped.

### Correlation Logic

Several procedures will now be given for associating detections with tracks. Of special interest are the conflicting situations of multiple tracks competing for a single detection or of multiple detections lying within a track's correlation gate (or region).

First, to limit the number of detections that can update a track, correlation gates are used. A detection can never update a track unless it lies within the correlation gate which is centered at the track's predicted position. The correlation gate should be defined in  $r\theta$  coordinates, regardless of what coordinate system is being used for tracking. Furthermore the gate size should be a function of the measurement accuracy  $R(t)$  and prediction error  $P(t|t-1)$  so that

\*A. L. Quigley and J. E. Holmes, "The development of Algorithms for the Formation and Updating of Tracks," Admiralty Surface Weapons Establishment, WP-XBC-7512, Portsmouth P06 4AA, Nov. 1975.

†G. V. Trunk, J. D. Wilson, B. H. Cantrell, J. J. Alter, and F. D. Queen, "Modifications to and Preliminary Results for the ADIT System," NRL Report 8091, Apr. 1977.

the probability of the correct detection lying with the gate is high (at least 0.99). In some tracking systems,\* the correlation gate is fed back to the automatic detector, and the detection threshold is lowered in the gate to increase  $P_D$ .

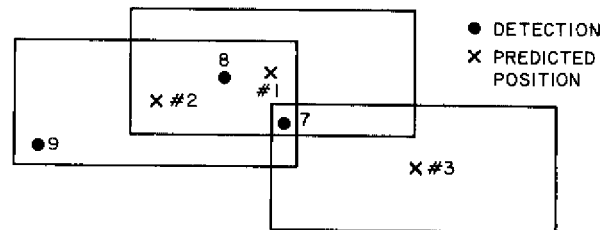
When several detections are within the correlation region, the usual and simplest solution is to associate the closest detection with the track. Specifically, the measure of closeness is the statistical distance

$$D^2 = \frac{(r_p - r_m)^2}{\sigma_r^2} + \frac{(\theta_p - \theta_m)^2}{\sigma_\theta^2}, \tag{77}$$

where  $(r_p, \theta_p)$  is the predicted position,  $(r_m, \theta_m)$  is the measured position,  $\sigma_r^2$  is the variance of  $r_p - r_m$ , and  $\sigma_\theta^2$  is the variance of  $\theta_p - \theta_m$ . Since the prediction variance is proportional to the measurement variance,  $\sigma_r^2$  and  $\sigma_\theta^2$  are sometimes replaced by the measurement variances. Statistical distance rather than Euclidean distance must be used, because the range accuracy is usually much better than the azimuth accuracy.

Problems associated with multiple detections and tracks are illustrated in Fig. 23: two detections are within gate 1, three detections are within gate 2, and one detection is within gate 3. Table 3 lists all detections within the tracking gate, and the detections are entered in the order of their statistical distance from the track. Tentatively, the closest detection is associated with each track, and then the tentative associations are examined to remove detections which are used more than once. Detection 8, which is associated with tracks 1 and 2, is paired with the closest track (track 1 in this case); then all other tracks are reexamined to eliminate all associations with detection 8. Detection 7 is tentatively associated with track 2; a conflict is noted but is resolved by pairing detection 7 with track 2. When other associations with detection 7 are eliminated, track 3 has no associations with it and consequently will not be updated on this scan. Thus track 1 is updated by detection 8, track 2 is updated by detection 7, and track 3 is not updated.

Fig. 23 — Example of the problems caused by multiple detections and tracks in close vicinity



An alternate strategy is to always pair a detection with a track if there is only one correlation with a track. As before, ambiguities are removed by using the smallest statistical distance. Thus track 3 in the example is updated by detection 7, track 1 is updated by detection 8, and track 2 is updated by detection 9.

\*S. R. Cook, "Development of IADT Tracking Algorithm," Johns Hopkins University, Applied Physics Laboratory, F3C-1-061, Sept. 1974.

Table 3 - Association Table for the Example shown in Fig. 23

Track Number	Closest Association		Second Association		Third Association	
	Detection Number	D <sup>2</sup>	Detection Number	D <sup>2</sup>	Detection Number	D <sup>2</sup>
1	8	1.2	7	4.2	-	-
2	8	3.1	7	5.4	9	7.2
3	7	6.3	-	-	-	-

Singer and Sea\* were two of the first people to recognize and characterize the interaction between the correlation and track update functions. Specifically, three distinct situations can occur: the track is not updated, the track is updated with the correct return, and the track is updated with an incorrect return. They generalized the tracking filter's error covariance equations to account for the a priori probability of incorrect returns being correlated with the track. This permits the analytical evaluation of tracking accuracy in a multitarget environment which produces false correlations. Furthermore, using the generalized tracking error covariance equation, they optimized the filter gain matrix, which yielded a new minimum-error tracking filter for multitarget environments. Also, they generated a suboptimal fixed-memory version of this filter to reduce computation and memory requirements.

A later paper by Singer et al.† uses a-posteriori correlation statistics based on all reports in the vicinity of the track. Again the mathematical structure is similar to the Kalman filter: the state equation is (58), the observation equation is (59), the one-step prediction is (60), and the corresponding covariance matrix is (61). The estimation error is denoted by  $\hat{X}(t|t') = \hat{X}(t) - X(t|t')$  and has mean and covariance matrices denoted by  $b(t|t')$  and  $P(t|t')$ . The correlation gate size and shape is based on the Mahalanobis distance,‡ and it is assumed  $n_k$  sensor reports fall within the gate on scan  $k$ . Included in the number  $n_k$  are extraneous reports whose number obeys a Poisson distribution and whose positions are uniformly distributed within the gate. The smooth estimate is given by

$$\hat{X}(t|t) = \hat{X}(t|t-1) + A(t), \quad (78)$$

where  $A(t)$  is chosen to minimize the noncentral second moment of the filter estimation error.

The problem is solved by using track histories. A track history  $\alpha$  at scan  $k$  is defined by selecting, for each scan  $i \leq k$ , a sensor report  $Y^{j_i}(i)$  where  $0 \leq j_i \leq n_i$ , with  $j_i = 0$  corresponding to the hypothesis that none of the reports belong to the track. The number of such track histories is

$$L(k) = \prod_{i=1}^k (1 + n_i). \quad (79)$$

\*R. A. Singer and R. G. Sea, IEEE Trans. Automatic Control AC-18, 571-582 (1973).

†R. A. Singer, R. G. Sea, and K. B. Housewright, IEEE Trans. Information Theory IT-20, 423-432 (1974).

‡R. A. Singer and A. J. Kanyuck, Automatica 7, 455-463 (1971).

Associated with each history  $\alpha$  is the probability  $p_{\alpha}(t)$  that the history  $\alpha$  is the correct one, given observations through time  $t$  (scan  $k$ ). The terms  $b_{\alpha}(t|t-1)$  and  $P_{\alpha}(t|t-1)$  are the bias and covariance of the estimation error  $\tilde{X}(t|t-1)$ , given observations through time  $t-1$  and given that track history  $\alpha'$  at time  $t-1$  is the (only) correct one. Recursive equations are obtained for  $p_{\alpha}$ ,  $b_{\alpha}$ , and  $P_{\alpha}$ ; then it is shown that the optimal correction vector is given by

$$A(t) = \sum_{\alpha=1}^{L(k)} p_{\alpha}(t) b_{\alpha}(t|t-1). \quad (80)$$

This solution not only minimizes the mean-square error but also is an unbiased estimate.

The trouble with the optimal a-posteriori filter is that it requires a growing memory. Hence several suboptimal filters were suggested. The first suboptimal filter considers only the last  $N$  scans; track histories which are identical for the last  $N$  scans are merged. The second suboptimal filter only considers the  $L$  nearest neighbors in the correlation gate; essentially the gate size is changed to limit number of reports to  $L$ . The last method uses both techniques: considers only the last  $N$  scans and restricts number of reports on any scan to  $L$ .

Simulations were run to compare the optimal and suboptimal a-posteriori filters, the optimal and suboptimal a-priori filters, and the Kalman filter. Some of the results are summarized in Figs. 24 and 25. In Fig. 24 the filter variance normalized by the theoretical (perfect-correlation) Kalman-filter variance is plotted for several filters. As a class the a-posteriori filters provide better performance than the other filters. However, for high density of false reports ( $4\beta\sigma_R^2 = 0.1$ ), the a-posteriori filter is 30 times worse than predicted by the standard Kalman-filter approach. Thus the standard approach should never be used in dense-target (or false-target) environments. Figure 25 gives the probability of making a false correlation. Again the a-posteriori filters provide the best performance.

Stein and Blackman\* have proposed a maximum-likelihood approach similar to Sittler† for solving the multitarget correlation problem. Their approach is unified in that they consider the total correlation-track problem which includes track initiation, confirmation, gating, and deletion logic. They compare their results with a standard approach and show significant performance improvements. However this author wonders how complicated the method is to implement and what their improvement is relative to a more sophisticated approach such as that of Singer et al.‡.

## Radar Integration

There are many ways of integrating (combining) radar detections from multiple radars into a single system track file. The type of radar integration that should be used is a function of the radar's performance and its environment. Although no firm rules can be generated, several methods and some general rules are as follows:

- Track selection. Generate a track with each radar, and choose one of the tracks for the system track. The only advantage of this method is that it is the simplest method to implement.

\*J. J. Stein and S. S. Blackman, IEEE Trans. Aerospace and Electronic Systems AES-11, 1207-1217 (1975).

†R. W. Sittler, IEEE Trans. Military Electronics ME-8, 125-139 (1964).

‡R. A. Singer, R. G. Sea, and K. B. Housewright, IEEE Trans. Information Theory IT-20, 423-432 (1974).

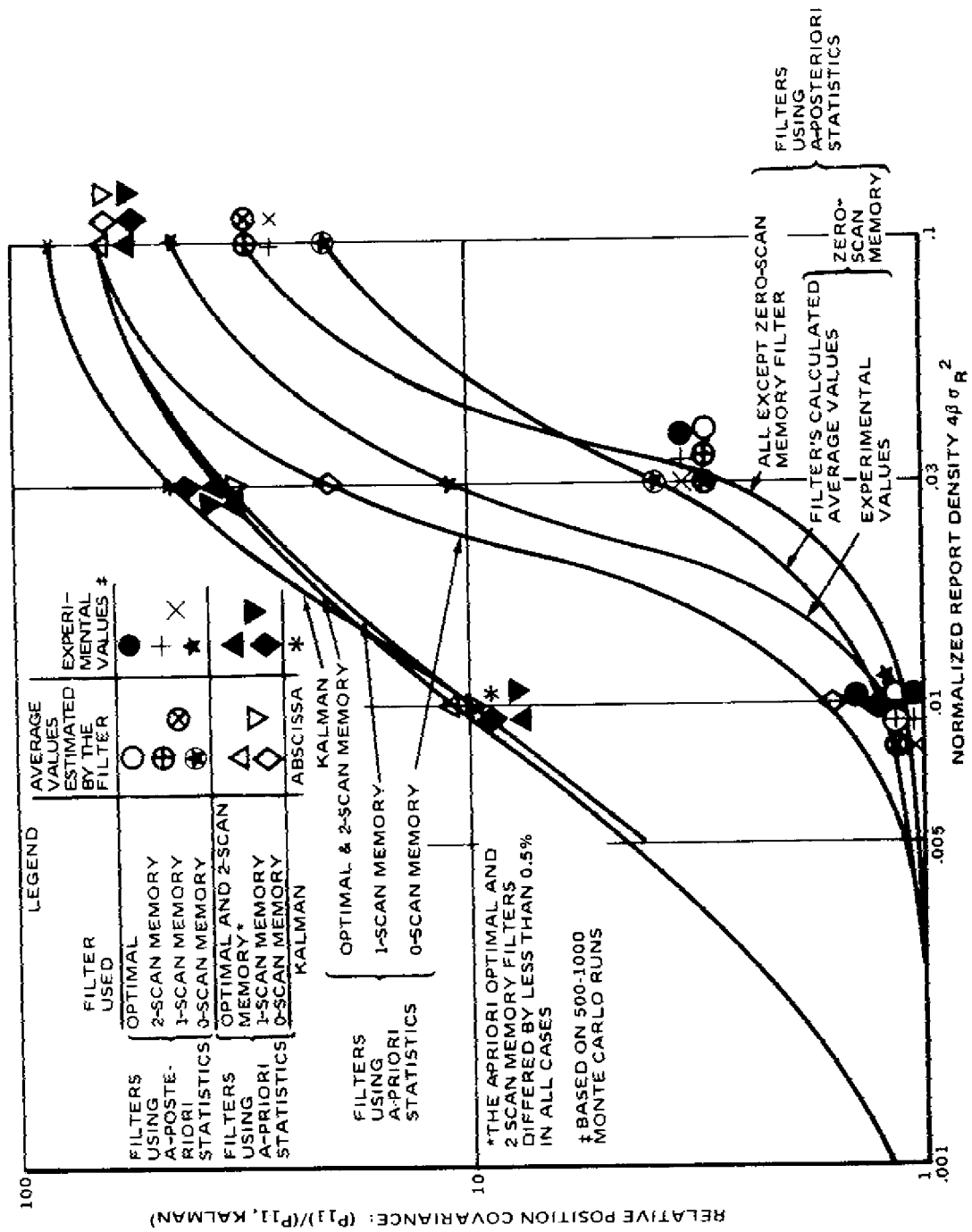


Fig. 24 — Experimental and calculated variances in filtered position errors for optimal and suboptimal a-posteriori and a-priori tracking filters. (From R. A. Singer, R. G. Sea, and K. B. Housewright, IEEE Trans. Information Theory IT-20, 423-432 (1974), courtesy of the Institute of Electrical and Electronics Engineers.)

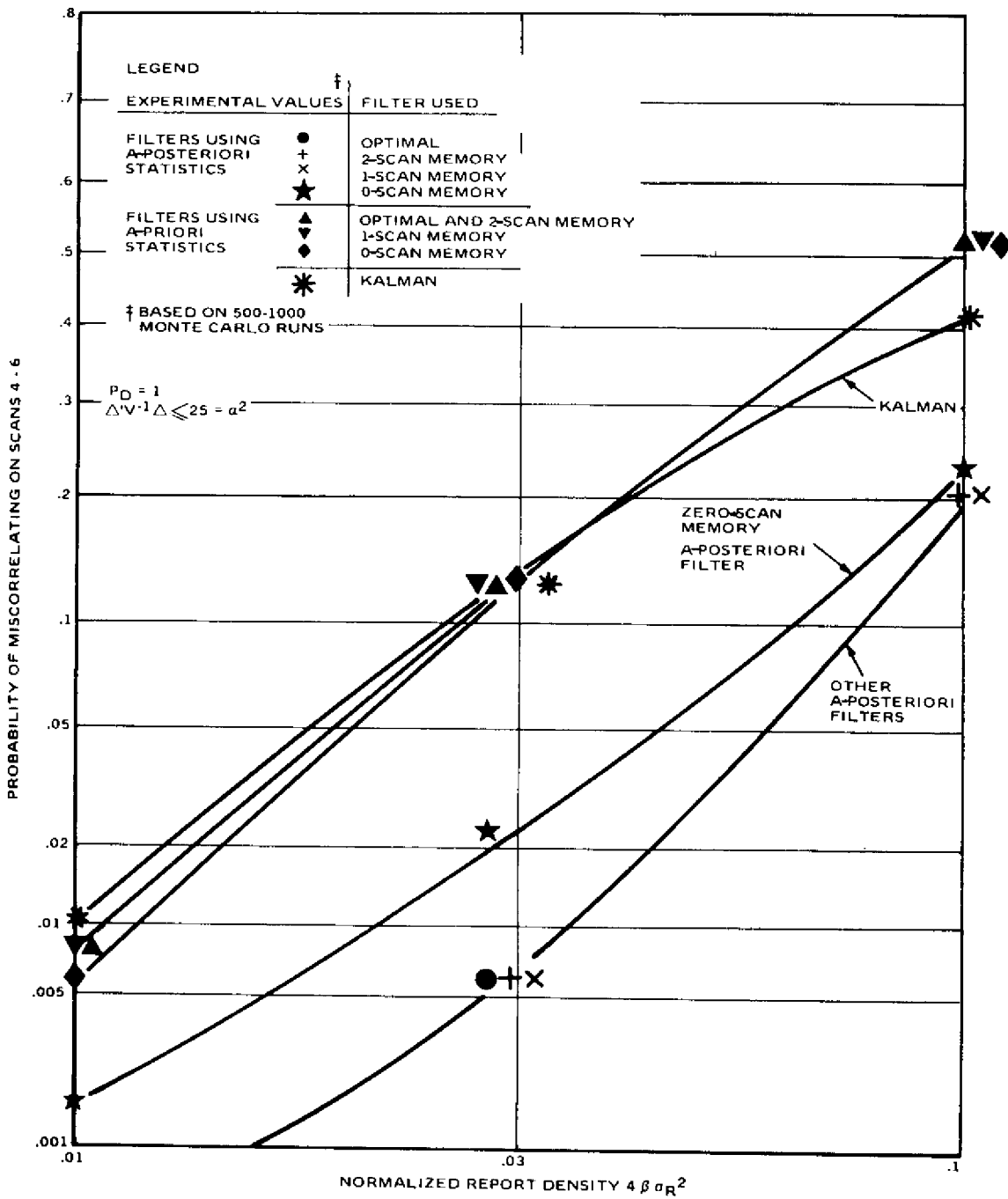


Fig. 25 — Experimental probability of divergence or lost track for optimal and suboptimal a-posteriori and a-priori tracking filters. (From R. A. Singer, R. G. Sea, and K. B. Housewright, IEEE Trans. Information Theory IT-20, 423-432 (1974), courtesy of the Institute of Electrical and Electronics Engineers.)

- Average track. Generate a track with each radar, and weight the tracks to form a system track. The method can be applied when many radars are providing unsynchronized radar data.
- Augmented track. Generate a track with each radar, choose one as the system track, but also use selected detections from other radars to update the system track. This method should be used when one radar provides substantially better data than other radars. Detections from other radars should be used when the primary radar misses some detections or when a target maneuver is declared.
- Average detection. Average all detections, and use the average to form a system track. This method should be used when many radars are providing detections essentially at the same instant.
- Merged detections. Use all detections to update the system track; tracks may or may not be initiated using all detections. Theoretically this method provides the most information; that is, if the detections are properly weighted, this method always provides the best performance. However care must be taken so that bad data do not corrupt good data. Thus this method should be used when the radars are supplying data of comparable accuracy.

The most important advantage of radar integration is provide the tracking information in one central source. Radar integration also provides improved track continuity and improved tracking performance on maneuvering targets. Little improvement is obtained in track-initiation times, since in practice almost always one radar will detect and establish a track before any other radar can provide some detections.

Either the  $\alpha - \beta$  filters or the Kalman filter can be used when the radars are at the same location. However Trunk and Wilson\* indicate that the Kalman filter must be used to provide triangulation effects when the radars are in different locations. Various methods for multiple-site correlation are also discussed by Singer and Kanyuck†.

## CONCLUDING REMARKS

The problems involved in coherent processing have received the greatest attention in this survey. Presently the trend appears to be toward a digital implementation of the adaptive processing algorithms: direct open-loop calculation of canceler weights and numerical inversion of the covariance matrix for adaptive arrays. It can be expected that such systems will be built and tested during the next several years.

The area of noncoherent processing has been studied intensively since 1940. The emphasis in later years has been on techniques to limit the number of false alarms (while suffering only a small target-sensitivity loss) so as not to overload the tracking system. Many systems have been built and tested, and not much more research seems necessary in this area.

---

\*G. V. Trunk and J. D. Wilson, "Tracking Filters for Multiple-Platform Radar Integration," NRL Report 8087, Dec. 1976.

†R. A. Singer and A. J. Kanyuck, *Automatica* 7, 455-463 (1971).

During the last several years much progress has been made in track-while-scan systems. This work has given guidance on the important problem of track-detection correlation in a dense multitarget environment. The major problem still needing a solution is that of track initiation in a dense environment.

One problem, which has received little attention so far but which will receive more attention, is that of adaptively controlling the surveillance radar. Problems of interest are: when should frequency and/or polarization diversity be used, when and where should various radar modes be used, and how should the signal processing be reconfigured to cope with a changing environment? Future radars will have more flexibility, and their control will become extremely important.